



OPEN

Heavy metal concentrations and pollution indicators in the Ennore ecosystem, east coast of Tamilnadu, India using atomic absorption spectrometry study with statistical approach

D. Rajendiran¹, N. Harikrishnan² & K. Veeramuthu³✉

The study of the heavy metals in the Ennore ecosystem plays a vital role in determining the extent of pollution in the area. Heavy metals such as Mg, Al, Si, K, Ca, Ti, Fe, V, Cr, Mn, Co Ni, Cu, Zn, As, Cd, Ba, La, and Pb were determined in twenty-six samples. The heavy metal concentration in the sediments was found to decrease in the sequence of Si > Al > Fe > Ca > Ti > K > Mg > Mn > Ba > V > Cr > Zn > La > Ni > Pb > Co > As > Cd > Cu in the study area, its varies as follows: 540–49,434, 3597–56,502, 22.37–691, 11.5–198.29, 69.10–1227.61, 1.40–19.95 and 11.48–38.63 for Ti, Fe, V, Cr, Mn, Co and Ni respectively. The average heavy metal concentrations were below the world's crustal average. The level of sediment pollution attributed to heavy metals was evaluated using several pollution indicators such as the enrichment factor (EF), contamination factor (CF), geoaccumulation index (I_{geo}), and pollution load index (PLI). The analysis, that revealed the average values of the enrichment factor indicates anthropogenic sources of Pb, Cr, As, Cd, Ni, V, Mn, and Zn. The average contamination factor (Cf) of metal Cd is slightly higher in some study areas (C2, B6, C10, B2, and S7). The results of the geoaccumulation index (I_{geo}) and pollution load index (PLI) indicate that the most of study area is not contaminated by heavy metals. The results of multivariate data analysis techniques, including Pearson correlation analysis, principal components, and clusters analysis, indicate that heavy metals in the sediments are of natural origin. This shows a general absence of serious pollution in the study area.

Keywords Ennore Creek, Sediments, Heavy metals, Atomic absorption spectrometry (AAS), Pollution indices, Statistical analysis

The rapid pace of urbanization and industrialization has exacerbated environmental pollution, emerging as a significant global concern recently¹. This issue is particularly pronounced in estuarine and coastal regions, where sediments are critical as major contaminants sink. Estuarine and coastal sediments serve as reservoirs for various pollutants, including heavy metals, due to their unique hydrodynamic and sedimentary processes. Suspended particulate matter in the water column accumulates heavy metals through adsorption and deposition. As these particles settle, they release trapped contaminants into the sediment matrix, leading to their accumulation over time².

The discharge of heavy metals into aquatic ecosystems results in their buildup in marine sediments, posing an ecological risk to filter-feeding organisms and eventually affecting humans^{3–7}. Although certain heavy metals like manganese, iron, copper, nickel, lead, and zinc are essential in trace amounts for their nutritional value, excessive exposure to these metals can be toxic and may lead to serious health conditions such as cancer, diabetes, asthma,

¹PG & Research Department of Physics, Shanmuga Industries Arts and Science College, Tiruvannamalai, Tamil Nadu 606603, India. ²Department of Physics, School of Arts and Science, Vinayaka Mission's Research Foundation (DU), Chennai Campus, Chennai, Tamil Nadu 603104, India. ³PG & Research Department of Physics, Thiru Kolanjiappar Government Arts College, Virudhachalam, Tamil Nadu 606001, India. ✉email: veera.kphysics@gmail.com

respiratory distress, cardiovascular diseases, and neurodegenerative disorders^{8,9}. Children, being particularly vulnerable to heavy metal(lloid)s, are exposed through additional pathways such as breastfeeding, placental transfer, hand-to-mouth activities during early childhood, and slower toxin elimination rates¹⁰. Moreover, chronic arsenic ingestion can result in lung conditions such as chronic bronchitis, chronic obstructive pulmonary disease, and bronchiectasis, as well as liver issues like non-cirrhotic portal fibrosis^{8,9}.

Measuring the concentration of heavy metals in soils, plants, waters, and sediments provides valuable information about the extent of environmental pollution and helps in implementing strategies to mitigate its adverse effects on both ecosystems and human health. Monitoring sediment contamination can also provide valuable information for managing and mitigating pollution in marine environments. Sediment-bound heavy metals tend to adsorb and accumulate on fine-grained particles that eventually move into the depositional areas¹¹.

Sediment pollution by heavy metals is regarded as a critical problem in marine environments because of their toxicity, persistence, and bioaccumulation^{12,13}. Many studies have shown that heavy metals in sediments can significantly negatively impact the health of marine ecosystems¹⁴. Knowledge of the distribution and concentration of heavy metals in sediments will help in detect their sources in aquatic systems¹⁵. Therefore, heavy metal distributions in sediments offer a more realistic approach to evaluating their actual environmental impact. The concentration of trace elements in coastal sediment can be useful for baseline studies and in the assessment of sediment quality in future research. Atomic absorption spectrometry (AAS) is an analytical technique used to determine the elemental composition of sediment samples. The AAS technique is a versatile tool commonly used in environmental research².

The study area, Ennore Port is situated on the Coromandel Coast of the Bay of Bengal, approximately 20 km north of Chennai city. Its strategic location makes it an important hub for regional trade and commerce. It handles a wide range of cargo, including coal, iron ore, petroleum products, containers, automobiles, and general cargo. Ennore Port has specialized terminals for handling different types of cargo, such as the coal terminal, liquid terminal, and container terminal. The area is dominated by intensive industrial activities with long-term effluent discharge into the river. This coast is a crucial environmental, economic, commercial, agricultural, and recreational location. This study was conducted to investigate whether the rapid economic development along the east coast of Tamilnadu had accelerated heavy metal pollution and to assess the potential ecological risk of sediment pollution by heavy metals. Specifically, the objectives of this study were: (1) to determine the levels of heavy metals (Mg, Si, Al, K, Ca, Ti, Fe, V, Cr, Mn, Co, Ni, Cu, As, Zn, Cd, Ba, La, and Pb) in the sediments (2) to quantify the extent of metal pollution using EF, I_{geo} , CF and PLI and (3) to identify possible sources of heavy metals by multivariate statistical methods. These indices offer a thorough evaluation of metal pollution levels, associated ecological risks, and potential impacts on aquatic ecosystems, supporting the prioritization of management strategies and guiding regulatory decision-making¹⁶.

Materials and methods

Study area

Ennore is home to the Ennore Port, officially known as Kamarajar Port Limited. This port serves as a major gateway for trade and commerce in the region, handling various types of cargo, including containers, coal, petroleum products, and general cargo. Ennore Port, with its strong maritime activity, is located on the east coast of the Indian peninsula in the Bay of Bengal, 2.5 km north of Ennore Creek¹⁷. The port plays a crucial role in facilitating maritime trade and industrial activities in the Chennai metropolitan area and surrounding regions. Ennore and its surrounding areas host several industrial facilities, including power plants, refineries, chemical industries, and manufacturing units¹⁸. These industries contribute to the local economy but also pose environmental challenges, such as pollution and ecological impacts on coastal ecosystems. Like many coastal areas undergoing rapid industrialization and urbanization, Ennore faces environmental challenges such as pollution of air, water, and soil, habitat degradation, and loss of biodiversity. Efforts are underway to address these concerns through pollution control measures, environmental regulations, and conservation initiatives. Despite industrialization, Ennore retains ecological significance due to its coastal habitats, including mangrove forests, estuaries, and tidal flats. These ecosystems provide critical habitats for various species of flora and fauna and play important roles in shoreline stabilization, water quality maintenance, and coastal resilience. Overall, Ennore is a dynamic area with a mix of industrial, commercial, and residential activities, alongside environmental and socioeconomic challenges that require careful management and sustainable development practices to ensure the well-being of both people and the environment. Table 1 gives the Geological information about the study area and Fig. 1 shows the Location map of the study area.

Sample collection and preparation

Figure 1 depicts the sample collection sites ($13^{\circ} 13' 18.50''$ N, $80^{\circ} 20' 10.10''$ E to $13^{\circ} 15' 13.33''$ N, $80^{\circ} 20' 17.43''$ E), while Table 1 provides geographical information for the locations. Sampling was conducted in compliance with standardized protocols to ensure representative and accurate data collection. A stratified random sampling approach was used to select sites across different zones of the study area, considering factors such as proximity to potential contamination sources (e.g., industrial sites, agricultural runoff, and urban areas). Sediment samples were collected at multiple depths to capture a representative profile of metal concentrations at different sediment layers. During the pre-monsoon season, 26 sediment samples were collected from the three different regions of Ennore such as sea (S), beach (B), and creek (C) regions on the east coast of Tamilnadu using a Peterson grab sampler. The sediment samples were collected from a distance of 10m parallel to the shoreline and 4m depth in the sea region (9 samples) and also the beach (8 samples) and creek regions (9 samples) of Ennore to examine the divergence of heavy metals from land to the marine environment. The selection of sites was based on a combination of environmental factors, including historical data on industrial activity, proximity to rivers

S. no.	Type of sample region	Sample ID	Latitude of location ID	Longitude of location ID
1	Sea	S1	13° 14' 46.02"	80° 20' 31.56"
2		S2	13° 14' 44.83"	80° 20' 48.04"
3		S3	13° 14' 44.09"	80° 21' 6.35"
4		S4	13° 14' 1.40"	80° 20' 20.71"
5		S5	13° 14' 1.32"	80° 20' 39.85"
6		S6	13° 14' 1.20"	80° 20' 56.76"
7		S7	13° 13' 18.50"	80° 20' 10.10"
8		S8	13° 13' 19.04"	80° 20' 29.96"
9		S9	13° 13' 19.54"	80° 20' 46.77"
10	Beach	B1	13° 15' 13.33"	80° 20' 17.43"
11		B2	13° 14' 49.77"	80° 20' 8.12"
12		B4	13° 14' 0.75"	80° 19' 46.26"
13		B5	13° 15' 12.59"	80° 20' 21.18"
14		B6	13° 14' 49.51"	80° 20' 10.55"
15		B7	13° 14' 0.79"	80° 19' 48.15"
16		B8	13° 15' 12.01"	80° 20' 25.27"
17		B9	13° 14' 49.51"	80° 20' 13.40"
18	Creek	C1	13° 13' 58.55"	80° 19' 38.62"
19		C2	13° 13' 50.50"	80° 19' 22.59"
20		C4	13° 13' 26.04"	80° 18' 53.16"
21		C5	13° 13' 9.64"	80° 18' 42.67"
22		C9	13° 13' 2.15"	80° 18' 52.99"
23		C10	13° 13' 59.38"	80° 18' 55.29"
24		C11	13° 14' 17.55"	80° 18' 56.60"
25		C12	13° 14' 35.42"	80° 18' 55.95"
26		C13	13° 14' 54.22"	80° 18' 51.95"

Table 1. Latitude and longitude of the study area of Ennore, east coast of Tamilnadu, India.

or discharge points, and ecological sensitivity. Sites with a history of pollution or high human activity were prioritized to better assess anthropogenic impacts. In contrast, control sites with minimal human influence were also included to understand background levels of contamination. Additionally, seasonal variations and tidal influences were taken into account. The sediment samples were transferred to polythene bags and properly labeled with the corresponding sampling site. Subsequently, these samples were transported to the laboratory and air-dried before manually picking out larger stone shards or shells. For the atomic absorption spectrometry study, the wet digestion method was used to digest the sediment samples. The samples were air-dried, ground, sieved through a 230 μ mesh sieve, and were accurately weighed to 2.5g into a digestion tube. For sample digestion, 10ml HNO₃ and 1ml H₂O₂ were added to the digestion tube. The digestion tubes were then placed in the digestive furnace and heated at 180°C for 3h. All the digests were cooled and filtered through Whatman (No.42) filter paper and then diluted to 50ml with double-distilled water 43. Each sample was digested in replicates of five, transferred to an acid-washed stoppered glass bottle, labeled, and kept for metal analysis.

Atomic absorption spectrometry analysis

In the present work, concentrations of heavy metals were determined using a Flame atomic absorption spectrometer (AAS, Analyst iCE3000, Thermo Scientific, USA). Qualitative and quantitative measurements of heavy metals were based on the absorption of optical radiation by atoms in the gaseous state 27. The standard solutions for all the heavy metals under study were prepared in three to five different concentrations to obtain a calibration curve by diluting a stock standard solution of a concentration of 1000ppm. Hollow cathode lamps for Pb, As, Hg, Cu, Zn, Cr, Ni, and Mn were used as radiation sources and the fuel was air acetylene. All the samples and standards were analyzed multiple times and the average value was taken as the result.

Results and discussion

Heavy metal concentration in surface sediments

The heavy metal concentration in surface sediments of a coastal area like Ennore can be influenced by various factors, including industrial activities, shipping, urbanization, and natural processes. Heavy metals are often introduced into sediments through industrial discharge, atmospheric deposition, urban runoff, and erosion of contaminated soils. Monitoring heavy metal concentrations in surface sediments is important for assessing environmental quality and potential risks to aquatic ecosystems and human health. Although these elements are essential for life, excessive amounts of these crucial metals can negatively affect the reproduction and metabolism of living organisms¹⁹. The concentration of elements in sediments from the study area is

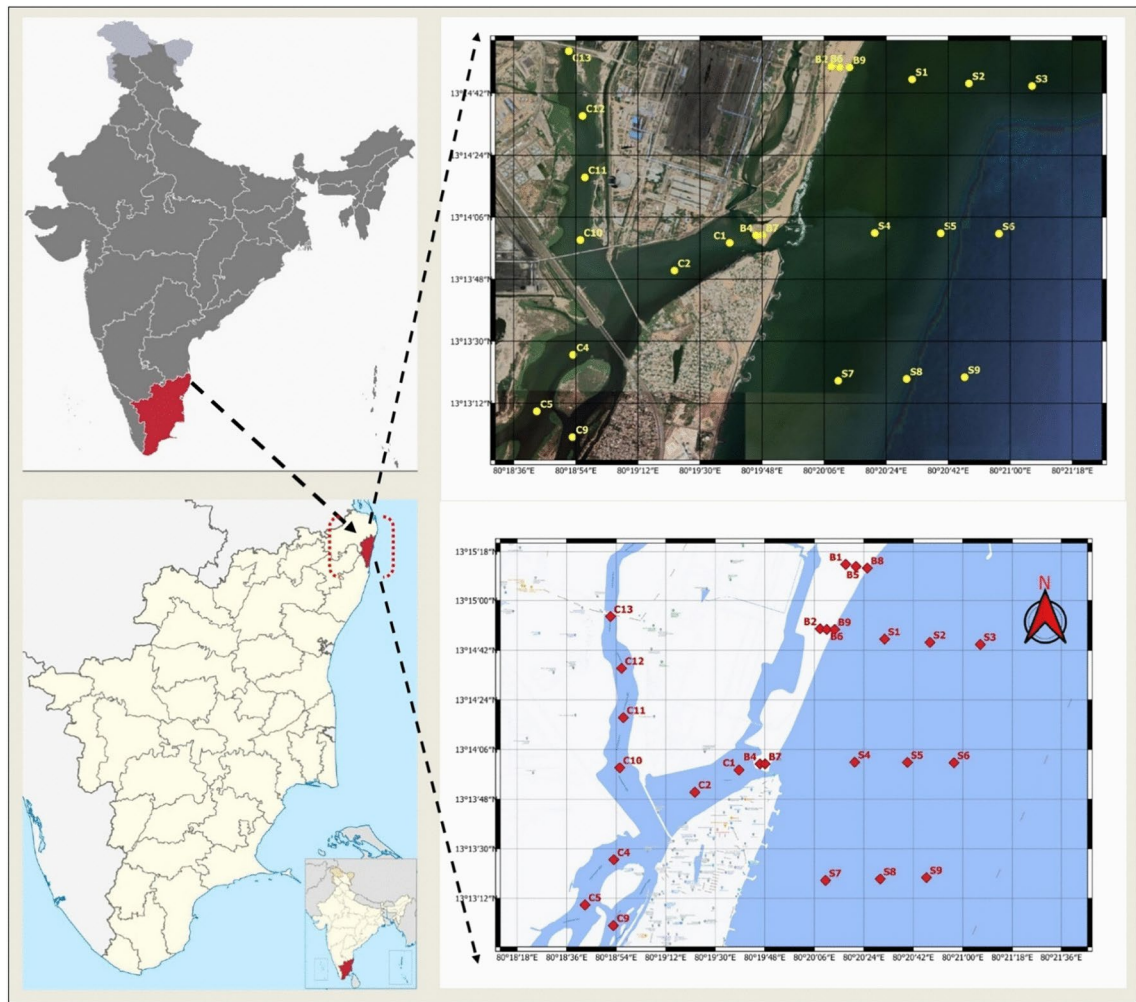


Fig. 1. Geographic overview of the study area. (The map was generated by QGIS geographic information system. Open source geospatial foundation project. Available at: <http://qgis.org>).

presented in Table 2. The concentration (mg kg^{-1}) varies as follows: 298–5987, 11,478–37,432, 115,987–224,978, 2985–9850, 3792–23,176, 540–49,434, 3597–56,502, 22,37–691, 11.5–198.29, 69.10–1227.61, 1.40–19.95, 11.48–38.63, BDL to 3.60, 11.04–87.99, 1.8–9.9, 1.1–11.2, 142.3–426.8, BDL to 214.7 and BDL to 30.7 for Mg, Al, Si, K, Ca, Ti, Fe, V, Cr, Mn, Co, Ni, Cu, Zn, As, Cd, Ba, La and Pb respectively. Among the heavy metals detected, Aluminum (Al), Iron (Fe), Calcium (Ca), Magnesium (Mg), and Silicon (Si) are the most abundant metals in the sediment, the mean concentrations of heavy metals were found in the following order: Si > Al > Fe > Ca > Ti > K > Mg > Mn > Ba > V > Cr > Zn > La > Ni > Pb > Co > As > Cd > Cu in the study area.

The locations of S2, S9, B4, B7, B9, C4, and C9 are characterized by higher concentrations of V, Cr, Co, Ni, and Zn when compared with other locations of the present study. This may be due to the high anthropogenic activities like harbor activities, industrial operations, urban waste discharges, and dredging, etc., The present findings are in agreement with the results from similar locations elsewhere²⁰. The studied elements, Ti, Fe, V, Cr, Mn, As, and Pb have high concentrations in the S1, S2, S9, B2, B7, B8, B9, C4, C5, C9, and C11 locations. This may be due to the activities of Ennore Port which handles various types of cargo, including coal, petroleum products, and general cargo. Port activities such as dredging, shipping, and cargo handling can disturb sediment layers and resuspend contaminants, contributing to the accumulation of heavy metals in sediments. Rare activities like ballast water discharge, oil spills, and accidental releases of hazardous materials from vessels, can introduce heavy metals into coastal waters and sediments. The Comparison of some heavy metal concentrations in sediments from this study with different regions are shown in Table 3 and variations in heavy metal concentration along the study area are shown in Fig. 2.

Quantification of heavy metal pollution in the sediments

Several methods are commonly used to assess heavy metal pollution in sediments, each providing valuable information about metal accumulation, distribution, and pollution status. Some of the key pollution indicators for quantitatively ranking different sampling sites include the enrichment factor (EF), geo-accumulation index (I_{geo}), contamination factor (CF), and pollution load index (PLI)^{21–23}. These pollution indicators are valuable

Sample ID	Element (Unit: ppm)												Pb					
	Mg	Al	K	Ca	Ti	V	Cr	Mn	Co	Ni	Cu	Zn	As	Cd	Ba	La		
S1	2822 ± 19.3	22,895 ± 215.40	4568 ± 14.6	23,176 ± 19.5	10,689 ± 842	30,771 ± 128.4	264,56 ± 17.6	113,33 ± 10.2	741,38 ± 44.1	12,95 ± 2.1	34,30 ± 1.6	1,69 ± 0.6	67,67 ± 6.5	4.5 ± 0.4	182,3 ± 14.5	30,0 ± 2.8	17.8 ± 1.7	
S2	4851 ± 28.1	30,132 ± 101.0	4950 ± 21.0	20,679 ± 14.6	1,8739 ± 44.6	40,889 ± 355.5	312,87 ± 20.6	145,77 ± 10.5	871,09 ± 49.5	16,35 ± 1.4	33,23 ± 2.6	3,60 ± 0.9	69,94 ± 5.9	8.4 ± 0.7	146,0 ± 13.2	49,2 ± 0.7	24.5 ± 2.1	
S3	840.0 ± 8.1	21,112 ± 111.5	2985 ± 11.4	10,057 ± 74.1	2,357 ± 9.4	98,94 ± 7.6	64,52 ± 4.1	249,11 ± 13.5	6,01 ± 0.9	13,21 ± 1.4	1,29 ± 0.1	29,78 ± 2.4	4.2 ± 0.1	2,7 ± 0.2	246,7 ± 18.5	17.1 ± 0.9	8.1 ± 0.9	
S4	1508 ± 17.0	12,066 ± 98.01	5192 ± 8.54	13,628 ± 55.9	3,976 ± 12.7	13,937 ± 124.6	78,38 ± 4.8	75,33 ± 1.6	264,74 ± 14.9	3,71 ± 0.1	27,58 ± 2.6	BDL	31,00 ± 3.1	3,7 ± 0.4	3,4 ± 0.3	226,1 ± 18.4	9.4 ± 0.4	7.1 ± 0.7
S5	805.0 ± 7.1	24,954 ± 156.2	7786 ± 14.9	14,363 ± 99.7	731 ± 7.1	8298 ± 78.9	37,85 ± 1.9	41,85 ± 2.0	159,81 ± 8.7	9,10 ± 1.0	26,84 ± 1.9	2,46 ± 0.1	234,7 ± 2.9	3,8 ± 0.1	21 ± 0.2	318,4 ± 19.5	1.9 ± 0.1	9.8 ± 0.8
S6	1842 ± 16.2	22,728 ± 124.5	9850 ± 13.2	10,586 ± 84.6	924 ± 6.8	6873 ± 66.5	23,12 ± 1.5	29,32 ± 1.1	138,35 ± 10.6	1,40 ± 0.8	19,67 ± 0.7	2,34 ± 0.3	39,023 ± 7.3	5.9 ± 0.6	1.9 ± 0.1	426,8 ± 32.8	BDL	4.6 ± 0.3
S7	1935 ± 14.9	21,075 ± 164.3	7047 ± 19.4	8403 ± 41.0	1,683 ± 14.6	9120 ± 17.9	41,01 ± 3.1	67,16 ± 3.8	165,61 ± 14.6	6,42 ± 0.6	22,16 ± 1.1	1,98 ± 0.1	26,08 ± 2.1	5.0 ± 0.4	3,8 ± 0.2	312,5 ± 19.4	3.9 ± 0.3	7.5 ± 0.9
S8	3355 ± 11.4	29,875 ± 109.1	4059 ± 984	17,169 ± 13.4	3769 ± 147.0	17,881 ± 15.9	96,6 ± 4.6	102,3 ± 7.4	132,3 ± 9.7	7,54 ± 1.0	28,1 ± 2.6	BDL	39,8 ± 3.4	4.5 ± 0.4	5.4 ± 0.4	290,4 ± 21.6	19.0 ± 1.1	6.0 ± 0.4
S9	4518 ± 35.2	25,067 ± 100.6	5932 ± 24.6	10,027 ± 97.5	8714 ± 74.6	24,994 ± 21.4	191,9 ± 11.2	148,1 ± 3.4	108,1 ± 8.9	7,31 ± 0.9	31,4 ± 2.0	2,65 ± 0.2	46,0 ± 4.1	7.0 ± 0.2	234,0 ± 19.4	9.0 ± 0.9	8.4 ± 0.6	
B1	895.0 ± 4.6	18,546 ± 98.44	7615 ± 12.8	9,643 ± 47.5	2,139 ± 18.4	9534 ± 68.7	77,11 ± 6.2	41,38 ± 3.2	190,26 ± 9.1	7,38 ± 1.3	18,86 ± 1.1	1,05 ± 0.5	27,54 ± 2.2	4.9 ± 0.3	298,4 ± 16.4	BDL	3.4 ± 0.1	
B2	844.0 ± 7.1	11,478 ± 87.02	6302 ± 10.3	7,939 ± 68.1	2,390 ± 11.6	8458 ± 74.1	48,9 ± 1.2	29,3 ± 1.6	177,1 ± 12.6	4,8 ± 0.8	12,8 ± 1.0	2,47 ± 0.2	21,0 ± 2.9	3,7 ± 0.2	3,1 ± 0.2	316,1 ± 28.4	28.1 ± 2.4	1.9 ± 0.1
B4	1942 ± 11.0	19,254 ± 144.3	4484 ± 8.65	7970 ± 44.2	49,434 ± 141.6	56,502 ± 447.6	691,0 ± 12.9	198,3 ± 11.6	122,76 ± 98.6	19,95 ± 1.6	27,4 ± 1.6	1,09 ± 0.1	87,99 ± 7.4	9.9 ± 0.9	2,9 ± 0.1	190,2 ± 14.6	214,7 ± 19.5	30.7 ± 2.9
B5	985.0 ± 6.5	20,147 ± 121.3	6844 ± 18.7	3,792 ± 17.9	1520 ± 107.6	3637 ± 288.6	22,4 ± 2.9	28,5 ± 1.9	72,1 ± 4.4	5,1 ± 0.6	19,2 ± 1.9	BDL	11,04 ± 1.0	5.0 ± 0.4	3,1 ± 0.2	420,9 ± 35.1	BDL	1.9 ± 0.1
B6	2447 ± 15.1	21,654 ± 210.6	7369 ± 25.9	6,806 ± 41.7	11,16 ± 84.6	7520 ± 84.6	26,37 ± 1.9	28,2 ± 1.1	128,05 ± 10.6	2,88 ± 0.8	11,48 ± 1.0	BDL	19,16 ± 1.2	3,8 ± 0.3	11,2 ± 1.1	335,4 ± 28.1	BDL	1.4 ± 0.1
B7	1974 ± 3.9	14,785 ± 144.6	5084 ± 17.4	17,809 ± 147.2	1,3,464 ± 119.5	22,269 ± 199.6	198,71 ± 0.6	129,00 ± 10.4	798,16 ± 47.9	18,81 ± 1.1	38,63 ± 3.6	2,04 ± 0.2	63,31 ± 6.4	3.5 ± 0.2	4,4 ± 0.4	210,0 ± 19.4	49.0 ± 4.6	18.0 ± 1.1
B8	889.0 ± 3.4	17,362 ± 173.1	4478 ± 11.4	20,176 ± 155.0	11,589 ± 105.4	33,441 ± 299.5	214,56 ± 17.6	113,33 ± 9.8	777,38 ± 68.4	16,95 ± 0.9	37,30 ± 2.9	1,9 ± 0.1	61,67 ± 5.8	6.8 ± 0.5	11 ± 0.1	162,3 ± 14.6	32.0 ± 1.1	21.8 ± 1.9
B9	1748 ± 1.6	21,568 ± 241.6	4350 ± 32.9	19,679 ± 146.1	18,539 ± 174.6	40,189 ± 400.9	330,87 ± 12.5	144,77 ± 12.4	899,09 ± 74.6	17,55 ± 1.6	31,23 ± 2.4	3,60 ± 0.3	69,94 ± 5.7	9.4 ± 0.9	1,2 ± 0.1	196,0 ± 12.6	50,2 ± 4.9	15.5 ± 1.1
C1	298.0 ± 4.4	13,132 ± 128.7	7100 ± 10.8	4,582 ± 10.3	540 ± 6.8	3597 ± 294.5	22,437 ± 1.8	11,5 ± 5.6	69,10 ± 5.9	2,10 ± 0.4	14,2 ± 1.6	BDL	12,0 ± 1.3	5.0 ± 0.4	2,4 ± 0.2	401,9 ± 39.4	BDL	BDL
C2	1166 ± 6.1	18,966 ± 176.1	7769 ± 21.7	7,396 ± 14.2	1,206 ± 11.9	5510 ± 51.6	22,21 ± 1.9	112,05 ± 9.8	2,88 ± 0.6	14,48 ± 1.1	2,11 ± 0.2	18,16 ± 1.4	3,8 ± 0.3	9.3 ± 1.1	275,4 ± 24.6	BDL	2.4 ± 0.2	
C4	5987 ± 1.1	30,733 ± 298.4	5144 ± 15.4	20,909 ± 447.0	14,964 ± 64.2	36,169 ± 311.0	224,71 ± 14.5	187,00 ± 15.8	748,16 ± 16.5	11,51 ± 1.1	31,63 ± 2.4	1,11 ± 0.1	61,31 ± 5.9	4.5 ± 0.4	4,1 ± 0.6	219,0 ± 18.4	45.0 ± 3.8	19.0 ± 1.5
C5	2945 ± 2.4	26,995 ± 256.3	4668 ± 9.87	20,976 ± 133.7	11,989 ± 113.7	34,071 ± 314.9	21,156 ± 11.0	111,33 ± 9.4	741,38 ± 14.6	10,95 ± 1.6	34,30 ± 2.8	1,98 ± 0.1	64,67 ± 5.1	1,8 ± 0.1	1,5 ± 0.1	142,3 ± 11.6	29.0 ± 1.9	14.6 ± 1.3
C9	4974 ± 6.4	37,432 ± 341.2	4750 ± 14.9	21,579 ± 211.2	18,939 ± 163.5	40,389 ± 394.6	309,87 ± 21.5	154,77 ± 9.7	871,09 ± 61.5	13,35 ± 1.1	31,23 ± 2.9	3,60 ± 0.4	61,94 ± 2.9	6.4 ± 0.5	2,5 ± 0.2	166,0 ± 14.6	55.2 ± 4.9	22.7 ± 2.0
C10	879.0 ± 11	22,112 ± 198.4	6185 ± 11.0	11,957 ± 97.8	3157 ± 32.8	12,807 ± 1118.4	61,94 ± 4.6	53,52 ± 3.5	241,11 ± 10.9	7,01 ± 0.6	24,21 ± 2.1	2,01 ± 0.3	29,78 ± 4.6	4,2 ± 0.4	4,9 ± 0.4	254,7 ± 19.4	21.6 ± 2.1	8.7 ± 0.9
C11	1598 ± 5.7	18,966 ± 166.6	5692 ± 19.5	11,528 ± 54.6	3676 ± 29.4	12,957 ± 99.7	98,38 ± 8.4	51,33 ± 2.8	261,74 ± 18.8	5,61 ± 0.7	22,59 ± 2.0	3,15 ± 0.4	28,00 ± 2.2	3,7 ± 0.3	3,5 ± 0.3	234,1 ± 19.4	7.9 ± 0.7	5.9 ± 0.1
C12	8020 ± 9.0	23,454 ± 199.2	7986 ± 10.1	10,963 ± 77.9	921 ± 7.9	8288 ± 74.6	30,85 ± 1.0	42,85 ± 1.6	147,81 ± 10.4	2,10 ± 0.6	24,84 ± 1.9	BDL	21,47 ± 2.7	5.8 ± 0.5	2,2 ± 0.2	309,2 ± 24.6	BDL	6.7 ± 0.6
C13	1801 ± 4.4	22,828 ± 211.5	9050 ± 18.5	11,986 ± 78.1	794 ± 6.6	6793 ± 51.2	27,12 ± 1.1	29,32 ± 1.1	122,35 ± 9.5	3,40 ± 0.9	22,67 ± 1.1	1,65 ± 0.2	39,02 ± 1.6	6.6 ± 0.4	1,7 ± 0.1	401,8 ± 38.4	2.5 ± 0.2	7.1 ± 0.7
Average	2101	21,899	6047	13,222	7998	19,526	144,86	83,24	400,58	8,56	25,14	168	41,19	5.3	3,55	266	26	10.6
Maximum	5987	37,432	9850	23,176	49,434	56,502	691.00	198,29	122,61	19,95	38,63	3,60	87,99	9.9	11.2	426,8	214,7	30.7
Minimum	298	11,478	2985	3792	540	3597	22,37	11.5	69,10	1,40	11,48	BDL	11,04	1.8	1.1	142,3	BDL	BDL

Table 2. Level of heavy metal concentration of the sediment samples along the study area.

S. no.	Area	Cr	Mn	Ni	Cu	Zn	Cd	Pb	References
1	Mediterranean Sea Coast, Northern, Cyprus	15–93	287–715	11–37	11–49	26–72	–	11–22	42
2	NE Mediterranean, Cyprus	9.0–46	141–1241	6.6–114	1.6–74	5.0–78	–	1.6–9.2	43
3	Ierissos Gulf, Greece	–	3835–25,982	–	31–206	936–4078	–	567–1698	44
4	Izmir Bay, Turkey	9–65	76–542	5–33	9–38	17–85	–	1–16	45
5	Nador Lagoon, Morocco	22.4–172.2	–	20.2–95.2	10.2–398.4	55.1–1250.0	–	15.6–326.2	46
6	Guadal, Spain	–	282–711	14–40	28–83	69–190	–	30–54	47
7	Gardon River, Southern France	–	–	–	–	43–1197	–	18–4476	48
8	Gulf of Tunis, Tunisia	15.55	–	14–51	1.5–19	27–450	–	16–107	49
9	Northern, Cyprus	55–144	112–990	44–245	9–127	29–128	–	1.1–24	50
10	Ennore Creek, Tamil Nadu, India	383	–	35	102	–	0.51	32	51
11	Cauvery Delta Region, Tamil Nadu, India	45.4–153.1	–	2.0–7.7	10.3–39.9	–	–	1.14–5.4	52
12	Mahanadi Estuary, East Central India	–	–	–	–	–	1.45	23.89	53
13	Arasalar Estuary, Tamil Nadu, India	0.44	–	0.8	–	–	3.9	0.19	54
14	Manakudy Estuary, Tamil Nadu, India	256.9–482.1	–	20.14–28.91	37.35–45.87	–	2.69–3.17	152.25–176.88	55
15	Romanian Sector, Black Sea	30.26	–	26.25	26.68	–	1.2	11.59	56
16	Daya Bay, China	–	–	–	30.6	–	0.28	52.7	57
17	Eastern Black Sea	5.6–56.9	–	16.1–21.4	4.43–122	–	3.8–5.9	41.7–355.1	58
18	Quanzhou Bay, Southeast China	37.1	–	10.3	19.8	–	0.24	42.2	59
19	Southwestern Coastal Rivers, Korea	29.1–128	–	11.3–44.3	3.2–68.6	–	0.1–0.82	11.9–79.2	60
20	Korean coast	–	–	–	0.18–104	–	0–1.37	0.04–85.4	61
21	Scheldt Estuary, Europe	41.6–161.4	–	10.8–45.5	18.6–118.4	–	1.51–10.24	–	62
22	Kerala Coast	–	–	25–80	7.0–38.0	–	0–1.9	4.0–30.0	63
23	Yangtze River Estuary, China	34.4	–	–	19.7	–	0.13	25.8	64
24	Yangtze River Estuary, China	69.5–103	–	18.8–38.9	14.3–32.1	–	0.037–0.212	13.7–23	65
25	Ennore Port, Tamilnadu, India (Present study)	83.24	400.58	25.14	1.68	41.19	3.55	10.68	(Present study)

Table 3. Comparison of some heavy metal concentrations in sediments from this study with different regions.

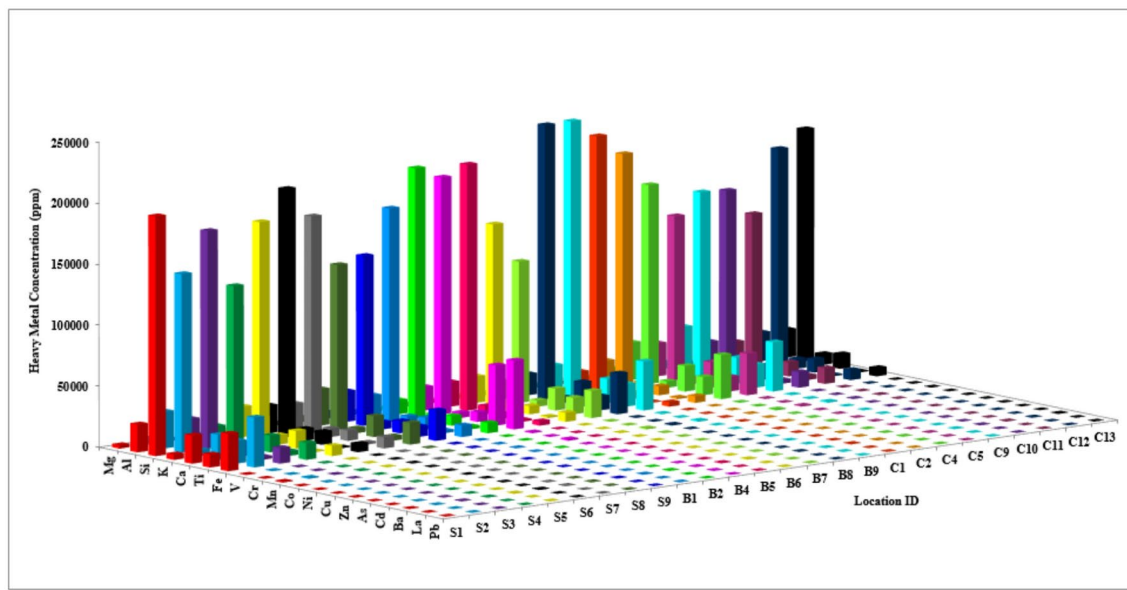


Fig. 2. Heavy metal concentration levels of sediments in the study area.

tools for assessing heavy metal pollution in sediments and prioritizing remediation efforts based on the relative contamination levels at different sampling sites. By applying these methods, researchers and environmental professionals can quantitatively rank sampling sites and inform decision-making processes aimed at mitigating the impacts of metal pollution on aquatic ecosystems and human health. Criteria of pollution indicators in sediment based on the EF, CF, and I_{geo} values are given in Table 4.

EF	Pollution status	CF	Pollution status	I_{geo}	Pollution status	Reference
> 1	With anthropogenic sources	≥ 6	Very high	> 5	Extreme	66
< 1	Without anthropogenic sources	3 ≤ CF < 6	Considerable	4–5	Strong to extremely strong	
		1 ≤ CF < 3	Moderate	3–4	Strong	
		< 1	Low	2–3	Moderate to strong	
				1–2	Moderate	
				0–1	Non-polluted to moderate	
				< 0	Non-polluted	

Table 4. Criteria of pollution indicators in sediment based on the EF, CF, and I_{geo} values.

Enrichment factor (EF)

The enrichment factor (EF) is a numerical indicator used to assess the degree of enrichment or depletion of a particular element or substance in a sample compared to a reference or background value. It is commonly applied in environmental studies, geochemistry, and mineral exploration to evaluate the extent of anthropogenic or natural enrichment of elements in soils, sediments, rocks, ores, and other materials. The EF for each element was calculated using the following formula (Eq. 1)^{24,25}.

$$EF = \left(\frac{C_x}{C_{Al}} \right)_{sample} / \left(\frac{C_x}{C_{Al}} \right)_{UCC} \quad (1)$$

where C_x and C_{Al} denote the concentrations of elements X and Al and EF is their ratio in the samples of interest to average shale obtained from Turekian and Wedepohl²⁶.

The Interpretation of the enrichment factor is as follows EF > 1 Indicates enrichment of the element or substance in the sample compared to the background/reference material, suggesting potential anthropogenic influence or natural enrichment processes, EF = 1 Indicates no enrichment or depletion, implying that the concentration of the element in the sample is similar to the background/reference value and EF < 1 Indicates depletion of the element or substance in the sample compared to the background/reference material, suggesting natural depletion processes or human activities reducing the concentration of the element. Generally, an EF value of < 1.5 suggests that such levels of metal enrichment might have originated entirely from crustal materials or natural weathering processes. An EF value of > 1.5 suggests that a significant portion of metal is delivered from non-crustal materials or non-natural weathering processes, so anthropogenic sources may become an important contributor^{22,27–29}. The enrichment factor (EF) levels of sediments in the study area are given in Table 5.

The average value of EF levels observed for heavy metals as follows: 0.53, 2.74, 1.00, 3.43, 7.07, 1.65, 6.66, 3.81, 1.87, 2.03, 2.11, 0.14, 1.78, 1.56, 46.94, 1.84, 1.08 and 1.93 for Mg, Si, K, Ca, Ti, Fe, V, Cr, Mn, Co, Ni, Cu, Zn, As, Cd, Ba, La and Pb respectively. The minimum EFs obtained for some elements (e.g., Mg, K, Cu, La, and Pb) are less than unity implying that these elements are depleted in some phases relative to crustal abundance in the study area. The EF values for Mg, K, Cu, and La were less than 1.5, which indicates dominant metal enrichments from natural sources in the study area. EF values greater than 1.5 that were obtained for Si, Ca, Ti, Fe, V, Cr, Mn, Co, Ni, Zn, As, Cd, Ba, and Pb suggest that these levels of enrichment might have originated from sources that are of non-crustal origin, including anthropogenic sources. The results observed are similar to those reported by Cheng and Hu³⁰. The heavy metal enrichment observed in sediments in Ennore, east coast of Tamilnadu, ranges from “minimal to moderate”. The order of EF values for all the elements is Cu < Mg < K < La < As < Fe < Zn < Ba < Mn < Pb < Co < Ni < Si < Ca < Cr < V < Ti < Cd. Variations in heavy metal enrichment factors along the study area are shown in Fig. 3.

Geo-accumulation index (I_{geo})

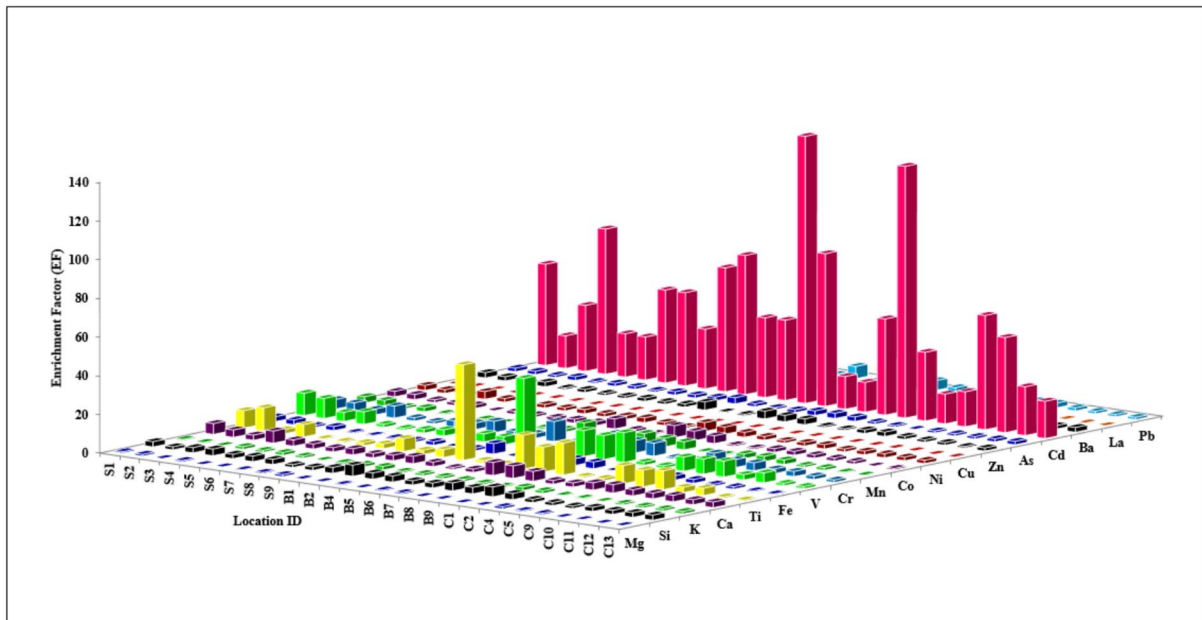
The geoaccumulation index (I_{geo}), introduced by Müller in 1979 and further elaborated in 1979, is a widely used method to assess the degree of metal enrichment in aquatic sediments. This index provides a quantitative measure of the contamination level of heavy metals in sediments relative to background levels. The formula for calculating the geoaccumulation index is as follows in Eq. (2)³¹.

$$I_{geo} = \log_2 \left(\frac{C_n}{1.5 \times B_n} \right) \quad (2)$$

where C_n is the concentration of metal “n” in the sediments, B_n is the background concentration value for metal “n” and factor 1.5 is used to account for possible variations in the background data due to lithological variations. The I_{geo} parameter was successfully calculated using the global average shale data^{26,32}.

According to the scale established by Muller³¹ and Mohit Aggarwal et al.³³, sediment can be classified as non-polluted ($I_{geo} < 0$), non-polluted to moderately polluted ($0 < I_{geo} < 1$), moderately polluted ($1 < I_{geo} < 2$), moderately to strongly polluted ($2 < I_{geo} < 3$), strongly polluted ($3 < I_{geo} < 4$) and strong to extremely polluted ($4 < I_{geo} < 5$) and extremely polluted ($I_{geo} > 5$). The I_{geo} values for each element at each sampling site were calculated using background values. The geo-accumulation index (I_{geo}) values for heavy metals at all the locations are given in Table 6.

S. No.	Sample ID	Mg	Si	K	Ca	Ti	Fe	V	Cr	Mn	Co	Ni	Cu	Zn	As	Cd	Ba	La	Pb
1	S1	0.73	2.74	0.67	5.62	8.98	2.49	11.56	4.95	3.24	2.83	2.63	0.13	2.74	1.81	52.41	1.10	1.14	3.11
2	S2	0.95	1.55	0.55	3.81	11.96	2.51	10.38	4.84	2.89	2.71	1.93	0.21	2.15	1.72	16.81	0.67	1.42	3.25
3	S3	0.23	2.7	0.47	2.65	2.15	1.12	4.69	3.06	1.18	1.42	1.10	0.11	1.31	1.21	34.10	1.61	0.71	1.53
4	S4	0.74	3.45	1.43	6.27	6.34	2.14	6.50	6.24	2.19	1.54	4.01	0.00	2.38	1.90	75.14	2.58	0.67	2.35
5	S5	0.19	2.3	1.04	3.2	0.56	0.62	1.52	1.68	0.64	1.82	1.89	0.18	0.87	0.94	22.44	1.76	0.07	1.58
6	S6	0.48	2.86	1.44	2.59	0.78	0.56	1.02	1.29	0.61	0.31	1.52	0.18	1.59	1.61	22.29	2.59	0.00	0.81
7	S7	0.54	2.7	1.11	2.22	1.54	0.80	1.95	3.19	0.79	1.52	1.84	0.17	1.15	1.44	48.08	2.05	0.16	1.43
8	S8	0.66	1.44	0.45	3.19	2.43	1.11	3.23	3.42	0.44	1.26	1.65	0.00	1.23	0.92	48.20	1.34	0.55	0.81
9	S9	1.06	1.78	0.79	2.22	6.69	1.85	7.65	5.91	0.43	1.45	2.20	0.19	1.70	1.71	30.85	1.29	0.31	1.34
10	B1	0.28	3.02	1.37	2.89	2.22	0.95	4.16	2.23	1.03	1.99	1.78	0.10	1.38	1.63	64.10	2.22	0.00	0.74
11	B2	0.43	5.71	1.83	3.84	4.00	1.36	4.26	2.56	1.54	2.07	1.96	0.38	1.69	1.96	72.02	3.80	2.13	0.67
12	B4	0.59	3.22	0.78	2.3	49.37	5.43	35.89	10.30	6.38	5.18	2.50	0.10	4.23	3.16	41.27	1.36	9.70	6.38
13	B5	0.29	3.2	1.13	1.05	1.45	0.33	1.11	1.41	0.36	1.27	1.68	0.00	0.51	1.51	41.56	2.88	0.00	0.38
14	B6	0.66	2.21	1.13	1.75	0.99	0.64	1.22	1.30	0.59	0.66	0.93	0.00	0.82	1.07	138.18	2.14	0.00	0.25
15	B7	0.79	2.51	1.15	6.69	17.51	2.79	13.44	8.73	5.40	6.26	4.58	0.25	3.96	1.46	78.96	1.96	2.88	4.86
16	B8	0.3	4.14	0.86	6.46	12.84	3.57	12.36	6.53	4.48	4.88	3.77	0.19	3.29	2.39	16.90	1.29	1.60	5.03
17	B9	0.48	3.33	0.67	5.07	16.53	3.45	15.34	6.71	4.17	4.02	2.54	0.30	3.00	2.68	15.46	1.25	2.02	2.87
18	C1	0.13	5.1	1.8	1.94	0.79	0.51	1.70	0.87	0.53	0.81	1.90	0.00	0.85	2.32	49.75	4.22	0.00	0.00
19	C2	0.36	3.23	1.37	2.17	1.22	0.54	1.28	1.17	0.59	0.76	1.34	0.20	0.89	1.22	130.20	2.00	0.00	0.51
20	C4	1.14	1.69	0.56	3.77	9.35	2.18	7.30	6.07	2.43	1.87	1.80	0.06	1.84	0.90	35.51	0.98	1.27	2.47
21	C5	0.64	1.59	0.58	4.32	8.54	2.34	7.84	4.12	2.75	2.03	2.23	0.13	2.22	0.40	15.41	0.73	0.93	2.16
22	C9	0.78	1.29	0.42	3.2	9.73	2.00	8.28	4.13	2.33	1.78	1.46	0.17	1.53	1.05	18.10	0.61	1.28	2.42
23	C10	0.23	2.16	0.93	3	2.75	1.07	2.80	2.42	1.09	1.59	1.92	0.16	1.25	1.16	59.09	1.59	0.85	1.57
24	C11	0.5	2.14	1	3.38	3.73	1.26	5.19	2.71	1.38	1.48	2.09	0.30	1.37	1.21	49.21	1.70	0.36	1.24
25	C12	0.2	2.42	1.13	2.6	0.76	0.65	1.32	1.83	0.63	0.45	1.86	0.00	0.85	1.52	25.24	1.82	0.00	1.14
26	C13	0.46	2.67	1.32	2.92	0.67	0.55	1.19	1.28	0.54	0.75	1.74	0.13	1.58	1.79	19.27	2.43	0.10	1.25
Average		0.53	2.74	1.00	3.43	7.07	1.65	6.66	3.81	1.87	2.03	2.11	0.14	1.78	1.56	46.94	1.84	1.08	1.93

Table 5. The enrichment factor levels of sediments in the study area.**Fig. 3.** Enrichment factor (EF) levels of sediments in the study area.

S. no.	Sample ID	Mg	K	Ca	Ti	Fe	V	Cr	Mn	Co	Ni	Zn	Cu	As	Cd	Ba	La	Pb
1	S1	-3	-3.13	-0.52	0.63	-1.2	0.44	-0.25	-0.78	-1.14	-1.57	-1.07	-5.32	-1.53	3.32	-2.25	-2.2	-0.75
2	S2	-2.21	-3.01	-0.68	1.44	-0.79	0.68	0.11	-0.55	-0.8	-1.62	-1.03	-4.23	-1.21	2.08	-2.58	-1.49	-0.29
3	S3	-4.74	-3.74	-1.72	-1.55	-2.47	-0.98	-1.07	-2.36	-2.25	-2.95	-2.26	-5.71	-2.22	0	-1.82	-3.01	-1.9
4	S4	-3.9	-2.94	-1.28	-0.8	-2.34	-1.32	-0.84	-2.27	-2.94	-1.89	-2.2	0	-2.39	0	-1.94	0	0
5	S5	-4.8	-2.36	-1.21	-3.24	-3.09	-2.37	-1.69	-3	-1.65	-1.93	-2.6	-4.78	-2.36	0	-1.45	0	-1.61
6	S6	-3.61	-2.02	-1.65	-2.9	-3.36	-3.08	-2.2	-3.2	-4.34	-2.37	-1.87	-4.85	-1.71	2.08	-1.03	0	-2.71
7	S7	-3.54	-2.5	-1.98	-2.04	-2.96	-2.25	-1.01	-2.94	-2.15	-2.2	-2.45	-5.09	-1.98	0	-1.48	-5.13	-1.99
8	S8	-2.75	-3.3	-0.95	-0.87	-1.99	-1.01	-0.4	-3.27	-1.93	-1.86	-1.84	0	-2.12	0	-1.58	-2.86	-2.31
9	S9	-2.32	-2.75	-1.73	0.34	-1.5	-0.02	0.13	-3.56	-1.97	-1.7	-1.63	-4.67	-1.48	0	-1.89	-3.94	-1.84
10	B1	-4.65	-2.39	-1.78	-1.69	-2.89	-1.34	-1.71	-2.74	-1.95	-2.43	-2.37	-6.01	-1.98	0	-1.54	0	-3.13
11	B2	-4.74	-2.66	-2.06	-1.53	-3.07	-2	-2.2	-2.85	-2.58	-2.99	-2.76	-4.77	-2.41	0	-1.46	0	-3.96
12	B4	-3.53	-3.15	-2.06	2.84	-0.33	1.83	0.55	-0.05	-0.51	-1.9	-0.7	-5.95	-0.98	2.73	-2.19	0.64	0.03
13	B5	-4.51	-2.54	-3.13	-2.18	-4.28	-3.12	-2.25	-4.14	-2.48	-2.41	-3.69	0	-1.97	2.8	-1.05	0	-3.98
14	B6	-3.2	-2.44	-2.28	-2.63	-3.23	-2.89	-2.26	-3.32	-3.31	-3.15	-2.89	0	-2.37	4.64	-1.38	0	-4.45
15	B7	-3.51	-2.97	-0.9	0.96	-1.67	0.03	-0.07	-0.68	-0.62	-1.4	-1.17	-5.05	-2.47	3.28	-2.05	-1.49	-0.74
16	B8	-4.66	-3.16	-0.72	0.75	-1.08	0.14	-0.25	-0.71	-0.75	-1.45	-1.21	-5.15	-1.53	1.29	-2.42	-2.11	-0.46
17	B9	-3.69	-3.2	-0.75	1.43	-0.82	0.76	0.1	-0.5	-0.72	-1.71	-1.03	-4.23	-1.05	1.47	-2.15	-1.46	-0.96
18	C1	-6.24	-2.49	-2.85	-3.68	-4.3	-3.12	-3.56	-4.21	-3.75	-2.84	-3.57	0	-1.97	2.44	-1.11	0	0
19	C2	-4.27	-2.36	-2.16	-2.52	-3.68	-3	-2.6	-3.51	-3.31	-2.82	-2.97	-5	-2.37	4.36	-1.66	0	-3.64
20	C4	-1.91	-2.96	-0.66	1.12	-0.97	0.2	0.47	-0.77	-1.31	-1.69	-1.22	-5.93	-2.11	3.19	-1.99	-1.62	-0.66
21	C5	-2.93	-3.1	-0.66	0.8	-1.06	0.12	-0.28	-0.78	-1.38	-1.57	-1.14	-5.09	-3.47	1.79	-2.61	-2.25	-1.04
22	C9	-2.18	-3.07	-0.62	1.46	-0.81	0.67	0.2	-0.55	-1.09	-1.71	-1.2	-4.23	-1.6	2.5	-2.39	-1.32	-0.41
23	C10	-4.68	-2.69	-1.47	-1.13	-2.47	-1.65	-1.33	-2.4	-2.02	-2.07	-2.26	-5.07	-2.22	3.44	-1.77	-2.67	-1.79
24	C11	-3.82	-2.81	-1.52	-0.91	-2.45	-0.99	-1.4	-2.28	-2.34	-2.18	-2.35	-4.42	-2.39	2.96	-1.89	-4.13	-2.35
25	C12	-4.81	-2.32	-1.6	-2.91	-3.09	-2.66	-1.66	-3.11	-3.77	-2.04	-2.73	0	-1.75	2.3	-1.49	0	-2.17
26	C13	-3.64	-2.14	-1.47	-3.12	-3.38	-2.85	-2.2	-3.38	-3.07	-2.17	-1.87	-5.35	-1.55	1.87	-1.11	-5.76	-2.07
Average		-3.76	-2.78	-1.48	-0.84	-2.28	-1.15	-1.06	-2.23	-2.08	-2.10	-2.00	-3.88	-1.97	1.87	-1.78	-1.57	-1.74
Minimum		-6.24	-3.74	-3.13	-3.68	-4.3	-3.12	-3.56	-4.21	-4.34	-3.15	-3.69	-6.01	-3.47	0	-2.61	-5.76	-4.45
Maximum		-1.91	-2.02	-0.52	2.84	-0.33	1.83	0.55	-0.05	-0.51	-1.4	-0.7	0	-0.98	4.64	-1.03	0.64	0.03

Table 6. Geo-accumulation index (I_{geo}) of the sediment in the study area.

The I_{geo} values of coastal sediments in the study area vary from -6.24 to -1.91 (-3.76) for Mg, -3.74 to -2.02 (-2.78) for K, -3.13 to -0.52 (-1.48) for Ca, -3.68 to 2.84 (-0.84) for Ti, -4.3 to -0.33 (-2.28) for Fe, -3.12 to 1.83 (-1.15) for V, -3.56 to 0.55 (-1.06) for Cr, -4.21 to -0.05 (-2.23) for Mn, -4.34 to -0.51 (-2.08) for Co, -3.15 to -1.4 (-2.10) for Ni, -3.69 to -0.7 (-2.00) for Zn, -6.01 to 0 (-3.88) for Cu, -3.47 to -0.98 (-1.97) for As, 0 to 4.64 (1.87) for Cd, -1.03 to -2.61 (-1.78) for Ba, -5.76 to 0.64 (-1.57) for La and -4.45 to 0.03 (-1.74) for Pb respectively (Table 6). The average I_{geo} values are given in parentheses. The average pollution degree of these metals decreased in the following order: Ti > Cr > V > Ca > La > Pb > Ba > Cd > As > Zn > Co > Ni > Mn > Fe > K > Mg > Cu. The average I_{geo} values (< 1) observed in the present study indicate no pollution of the investigated metals in the sampling locations of the study area. The variation of I_{geo} values with the locations is shown in Fig. 4.

Contamination factor (CF)

The contamination factor (CF) is another widely used index in environmental geochemistry to assess the degree of heavy metal contamination in sediments. It provides a quantitative measure of the contamination level relative to background or reference values. The CF is calculated using the following Eq. (3).

$$CF = \frac{C_{\text{heavymetal}}}{C_{\text{background}}} \quad (3)$$

' $C_{\text{background}}$ ' refers to the concentration of metal of interest in the sediments when there was no anthropogenic input. $CF < 1$ indicates low contamination by a metal, $1 < CF < 3$ indicates moderate contamination, $3 < CF < 6$ implies considerable contamination, and $CF > 6$ denotes high contamination^{34,35}.

The contaminant factor (CF) in sediments from the study area is presented in Table 8. The results of CF values are 0.13–0.43 (average 0.25) for Al, 0.02–0.4 (average 0.14) for Mg, 0.11–0.37 (average 0.23) for K, 0.24–1.45 (average 0.83) for Ca, 0.12–10.75 (average 1.74) for Ti, 0.08–1.2 (average 0.41) for Fe, 0.17–5.32 (average 1.12) for V, 0.13–2.2 (average 0.93) for Cr, 0.08–1.44 (average 0.47) for Mn, 0.08–1.44 (average 0.45) for Co, 0.23–0.77 (average 0.50) for Ni, 0.12–0.43 (average 0.50) for Zn, 0–0.08 (average 0.04) for Cu, 0.14–0.76 (average 0.41) for As, 3.36–37.4 (average 11.85) for Cd, 0.25–0.74 (average 0.46) for Ba, 0–2.33 (average 0.28) for La and 0–1.53 (average 0.53) for Pb respectively with the order of Cd > Ti > V > Cr > Ca > Pb > Ni > Mn > Ba > Co > Zn > Fe > As > La > Al > K > Mg > Cu.

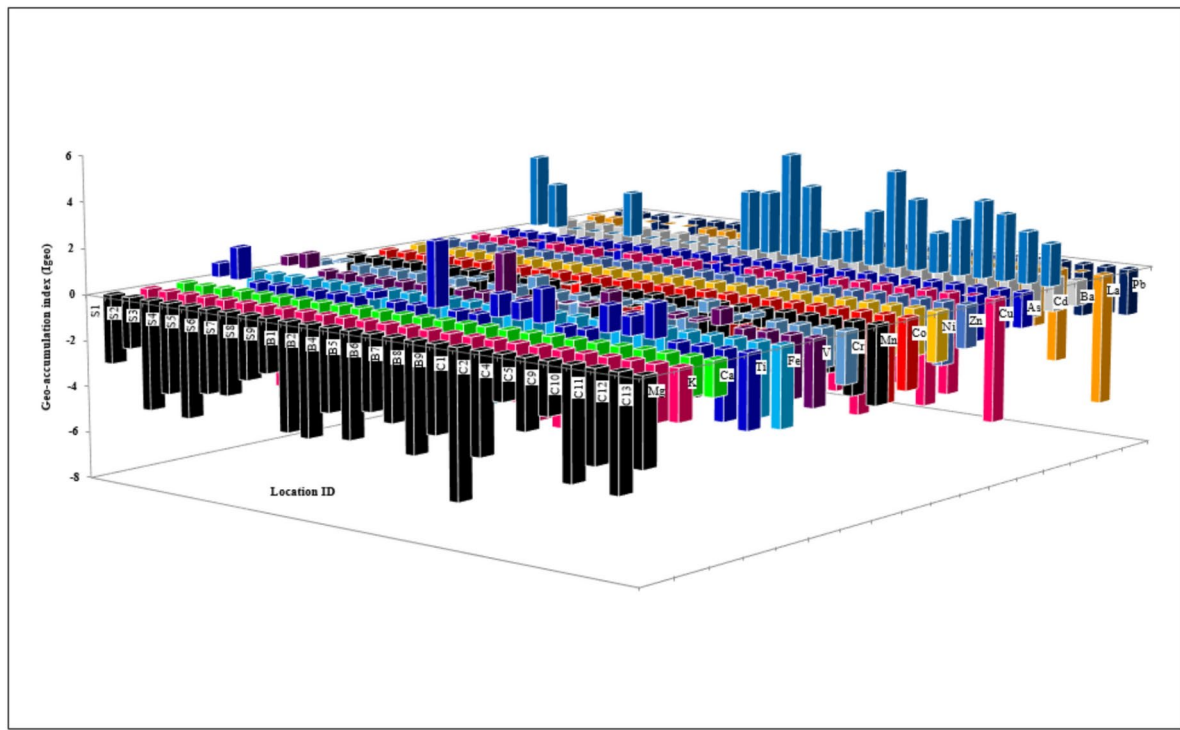


Fig. 4. Geo-accumulation index (I_{geo}) of the sediment in the study area.

The average CF value for element Cd indicates extreme contamination, while Ti and V indicate moderate contamination. The other elements Al, Mg, K, Ca, Cr, Mn, Co, Ni, Zn, Cu, As, Ba, La, and Pb indicate low contamination. High contamination levels were observed in the locations for Cd S4 - 11.33; S7 - 12.67; B1- 14.86; B2 - 10.33; B4 - 9.93; B5 - 10.47; B6 - 37.4; B7 - 14.59; C2 - 30.87; C4 - 13.67; C10 - 16.33 and C11 - 11.67 for Cd. The accumulation of heavy metals in sediment samples can arise from various sources, both natural and anthropogenic. Common sources contributing to heavy metal accumulation in sediments include municipal wastewater discharge, mining activities, agricultural activities, and drainage rivers and creeks^{30,36}. The variation of CF values with the locations is shown in Fig. 5.

Pollution load index (PLI)

The pollution load index (PLI) is a comprehensive index used to evaluate the overall pollution status of heavy metals in sediment samples. It integrates multiple heavy metal concentrations to provide a single numerical value that represents the pollution load in sediments. The PLI is calculated using the following Eq. (4):

$$PLI = (CF_1 \times CF_2 \times CF_3 \times \dots \times CF_n)^{1/n} \quad (4)$$

where CF_n is the value of the CF for metal n. The PLI values were interpreted as follows: polluted ($PLI > 1$), unpolluted ($PLI < 1$), and moderated ($PLI = 1$)³⁷. The PLI value of zero indicates “no pollution”. The PLI results range from 0.25 to 1.03 with an average mean value of 0.49, thus indicating that the study area is practically not polluted. Table 7 gives the contamination factor (CF) and pollution load index (PLI) values for the study area. Figure 6 shows the variation in the contamination factor (CF) values of heavy metals and the pollution load index (PLI) with locations.

Multivariate statistical analysis

Pearson correlation analysis

Correlation is a statistical tool that helps to measure and analyze the degree of relationship between two variables. The degree of relationship between the variables under consideration is measured through correlation analysis³⁸. The correlation measure is called the correlation coefficient, which ranges from correlation ($-1 \leq r \geq +1$). A sign indicates the direction of change. Correlation analysis gives us an idea about the degree and direction of the relationship between the two variables under this study.

The correlation coefficients determined based on the results of element analyses of beach sediments are presented in Table 8. The correlation coefficient was calculated using Pearson correlation. The following elements were found to have strong positive correlations (at the 0.01 level) with the other elements mentioned: Mg with Al, Ca, Fe, Cr, Ni and Zn; Ca with Fe, Cr, Mn, Co and Ni; Fe with V, Cr, Mn, Co, Ni, Zn and As; On the other hand, high negative correlations (at the 0.01 level) were found between Ca, Ti, Fe, V, Cr, Mn, Co, Ni, Zn and Ba. Ca constitutes a different origin group from Si. Metals showing a high positive correlation were interpreted to

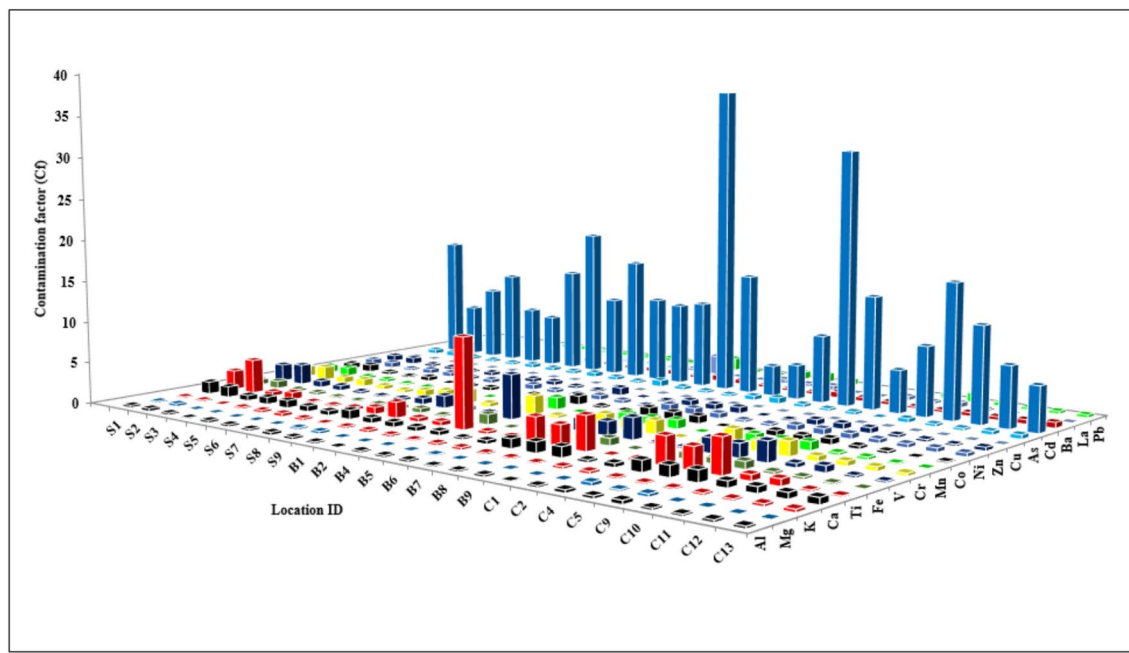


Fig. 5. Contamination factor (Cf) of the study area.

S. no.	Sample ID	Al	Mg	K	Ca	Ti	Fe	V	Cr	Mn	Co	Ni	Zn	Cu	As	Cd	Ba	La	Pb	PLI
1	S1	0.26	0.19	0.17	1.45	2.32	0.65	2.04	1.26	0.87	0.68	0.69	0.71	0.04	0.52	15	0.31	0.33	0.89	0.67
2	S2	0.34	0.32	0.19	1.29	4.07	0.87	2.41	1.62	1.02	0.86	0.66	0.74	0.08	0.65	6.33	0.25	0.53	1.22	0.86
3	S3	0.24	0.06	0.11	0.63	0.51	0.27	0.76	0.72	0.29	0.32	0.26	0.31	0.03	0.32	9	0.43	0.19	0.4	0.36
4	S4	0.14	0.1	0.2	0.85	0.86	0.3	0.6	0.84	0.31	0.2	0.55	0.33	-	0.29	11.33	0.39	0.1	0.35	0.44
5	S5	0.28	0.05	0.29	0.9	0.16	0.18	0.29	0.47	0.19	0.48	0.54	0.25	0.05	0.29	7	0.55	0.02	0.49	0.38
6	S6	0.26	0.12	0.37	0.66	0.2	0.15	0.18	0.33	0.16	0.07	0.39	0.41	0.05	0.46	6.33	0.74	-	0.23	0.38
7	S7	0.24	0.13	0.26	0.53	0.37	0.19	0.32	0.75	0.19	0.34	0.44	0.27	0.04	0.38	12.67	0.54	0.04	0.38	0.34
8	S8	0.34	0.22	0.15	1.07	0.82	0.38	0.74	1.14	0.16	0.39	0.56	0.42	-	0.35	18	0.5	0.21	0.3	0.45
9	S9	0.28	0.3	0.22	0.63	1.89	0.53	1.48	1.65	0.13	0.38	0.63	0.48	0.06	0.54	9.67	0.4	0.1	0.42	0.5
10	B1	0.21	0.06	0.29	0.6	0.47	0.2	0.59	0.46	0.22	0.39	0.38	0.29	0.02	0.38	14.86	0.51	-	0.17	0.38
11	B2	0.13	0.06	0.24	0.5	0.52	0.18	0.38	0.33	0.21	0.25	0.26	0.22	0.05	0.28	10.33	0.55	0.31	0.1	0.32
12	B4	0.22	0.13	0.17	0.5	10.75	1.2	5.32	2.2	1.44	1.05	0.55	0.93	0.02	0.76	9.93	0.33	2.33	1.53	1.03
13	B5	0.23	0.07	0.26	0.24	0.33	0.08	0.17	0.32	0.08	0.27	0.38	0.12	-	0.38	10.47	0.73	-	0.1	0.31
14	B6	0.25	0.16	0.28	0.43	0.24	0.16	0.2	0.31	0.15	0.15	0.23	0.2	-	0.29	37.4	0.58	-	0.07	0.29
15	B7	0.17	0.13	0.19	1.11	2.93	0.47	1.53	1.43	0.94	0.97	0.77	0.67	0.05	0.27	14.59	0.36	0.53	0.9	0.62
16	B8	0.2	0.06	0.17	1.26	2.52	0.71	1.65	1.26	0.91	0.89	0.75	0.65	0.04	0.52	3.67	0.28	0.35	1.09	0.63
17	B9	0.25	0.12	0.16	1.23	4.03	0.85	2.55	1.61	1.06	0.91	0.62	0.74	0.08	0.73	4.17	0.34	0.55	0.77	0.74
18	C1	0.15	0.02	0.27	0.29	0.12	0.08	0.17	0.13	0.08	0.11	0.28	0.13	-	0.38	8.17	0.69	-	-	0.25
19	C2	0.22	0.08	0.29	0.46	0.26	0.12	0.19	0.25	0.13	0.15	0.29	0.19	0.05	0.29	30.87	0.47	-	0.12	0.28
20	C4	0.35	0.4	0.19	1.31	3.25	0.77	1.73	2.08	0.88	0.61	0.63	0.65	0.02	0.35	13.67	0.38	0.49	0.95	0.73
21	C5	0.31	0.2	0.18	1.31	2.61	0.72	1.63	1.24	0.87	0.58	0.69	0.68	0.04	0.14	5.2	0.25	0.32	0.73	0.59
22	C9	0.43	0.33	0.18	1.35	4.12	0.86	2.38	1.72	1.02	0.7	0.62	0.65	0.08	0.49	8.47	0.29	0.6	1.13	0.77
23	C10	0.25	0.06	0.23	0.75	0.69	0.27	0.48	0.59	0.28	0.37	0.48	0.31	0.04	0.32	16.33	0.44	0.24	0.44	0.39
24	C11	0.22	0.11	0.21	0.72	0.8	0.27	0.76	0.57	0.31	0.3	0.45	0.29	0.07	0.29	11.67	0.4	0.09	0.3	0.37
25	C12	0.27	0.05	0.3	0.69	0.2	0.18	0.24	0.48	0.17	0.11	0.5	0.23	-	0.45	7.4	0.53	-	0.33	0.34
26	C13	0.26	0.12	0.34	0.75	0.17	0.14	0.21	0.33	0.14	0.18	0.45	0.41	0.04	0.51	5.5	0.69	0.03	0.36	0.3
Average		0.25	0.14	0.23	0.83	1.74	0.41	1.12	0.93	0.47	0.45	0.50	0.43	0.04	0.41	11.85	0.46	0.28	0.53	0.49
Minimum		0.13	0.02	0.11	0.24	0.12	0.08	0.17	0.13	0.08	0.07	0.23	0.12	0	0.14	3.67	0.25	0	0	0.25
Maximum		0.43	0.4	0.37	1.45	10.75	1.2	5.32	2.2	1.44	1.05	0.77	0.93	0.08	0.76	37.4	0.74	2.33	1.53	1.03

Table 7. Contamination factor (CF) and pollution load index (PLI) of the study area.

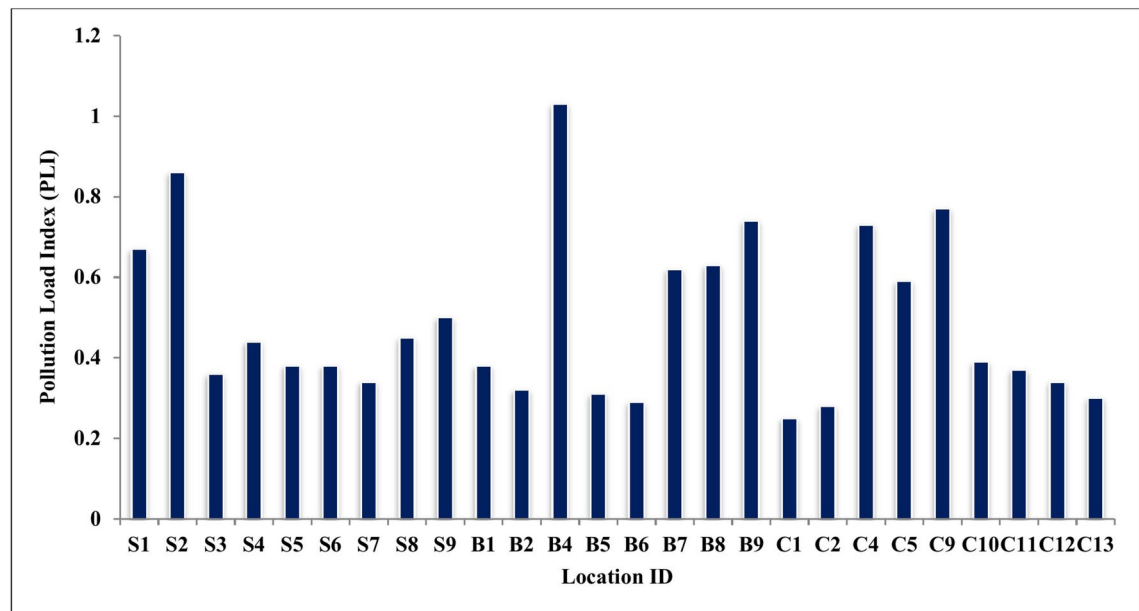


Fig. 6. Pollution load index (PLI) of the study area.

Variables	Mg	Al	Si	K	Ca	Ti	Fe	V	Cr	Mn	Co	Ni	Cu	Zn	As	Cd	Ba
Mg	1																
Al	0.756	1															
Si	-0.437	-0.271	1														
K	-0.330	-0.166	0.239	1													
Ca	0.570	0.530	-0.223	-0.533	1												
Ti	0.388	0.212	0.017	-0.519	0.339	1											
Fe	0.587	0.418	-0.060	-0.669	0.655	0.907	1										
V	0.422	0.253	0.016	-0.598	0.432	0.984	0.946	1									
Cr	0.710	0.459	-0.217	-0.682	0.647	0.832	0.938	0.867	1								
Mn	0.432	0.272	-0.003	-0.623	0.670	0.881	0.940	0.904	0.845	1							
Co	0.361	0.227	-0.021	-0.647	0.648	0.808	0.873	0.843	0.831	0.920	1						
Ni	0.502	0.372	-0.279	-0.480	0.828	0.504	0.707	0.561	0.759	0.694	0.757	1					
Cu	0.297	0.298	-0.016	-0.135	0.429	0.249	0.392	0.307	0.326	0.389	0.428	0.342	1				
Zn	0.558	0.374	-0.069	-0.574	0.731	0.842	0.944	0.887	0.896	0.930	0.878	0.784	0.423	1			
As	0.216	0.196	0.432	-0.139	0.166	0.631	0.588	0.660	0.505	0.504	0.501	0.303	0.282	0.567	1		
Cd	0.018	-0.079	-0.252	0.146	-0.302	-0.217	-0.299	-0.251	-0.250	-0.285	-0.290	-0.416	-0.323	-0.335	-0.361	1	
Ba	-0.463	-0.290	0.334	0.780	-0.729	-0.615	-0.810	-0.691	-0.772	-0.783	-0.755	-0.702	-0.445	-0.751	-0.206	0.136	1

Table 8. Pearson correlation coefficients among heavy metals of sediments from study area. Significant values are in [bold]. **Correlation is significant at the 0.01 level (2-tailed). *Correlation is significant at the 0.05 level (2-tailed).

be of similar origin^{38,39}. These metals were found to be associated with Si. However, the elements with negative correlations were thought to have different origins. Figure 7 shows the Pearson correlation coefficients among heavy metals present in the study area.

Principal component analysis

Principal component analysis (PCA) is widely used to transform many variables into a small number of significant variables. This method calculates the maximum common variance using all variables, which are then put into a common factor. According to its purpose, factor analysis is divided into two methods: exploratory and confirmatory³⁴. Exploratory factor analysis is preferred when a theory is suggested by finding a factor using the relationship between variables; conversely, confirmatory factor analysis is selected when the relationship between variables will be used to test a previously known theory.

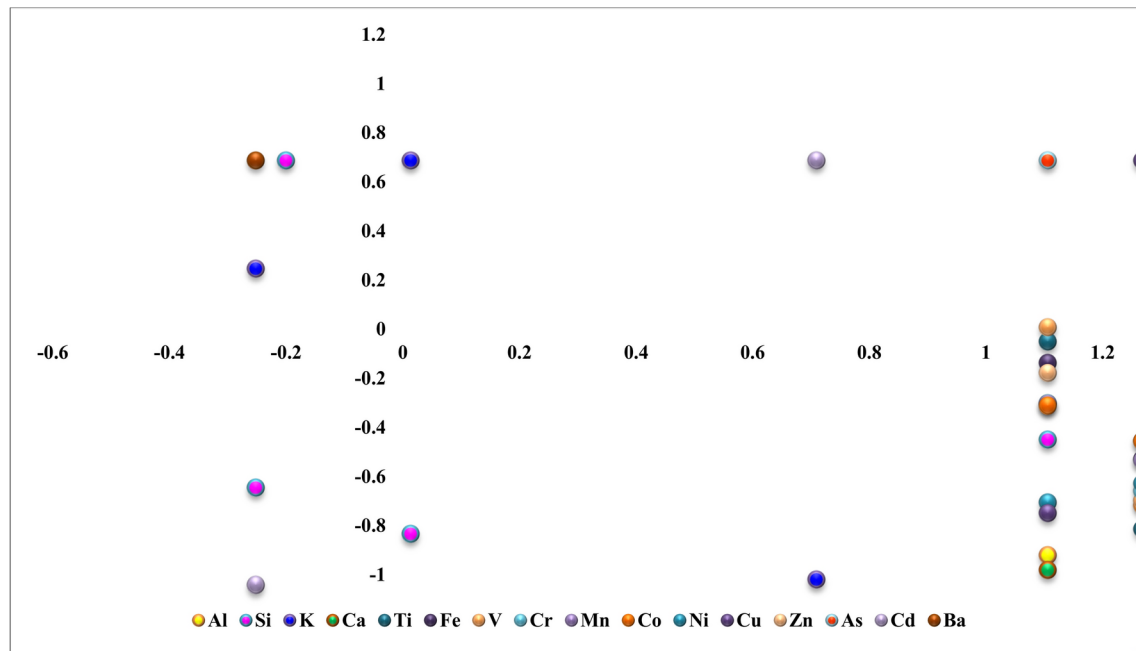


Fig. 7. Pearson correlation coefficients among heavy metals of sediments.

Variables	Component 1	Component 2
Mg	0.703	-0.046
Al	0.489	0
Si	-0.576	0.818
K	-0.652	-0.167
Ca	0.629	0.161
Ti	0.755	0.557
Fe	0.848	0.523
V	0.779	0.572
Cr	0.88	0.353
Mn	0.774	0.542
Co	0.726	0.487
Ni	0.711	0.155
Cu	0.316	0.198
Zn	0.808	0.483
As	0.263	0.715
Cd	-0.102	-0.377
Ba	-0.815	-0.164
La	0.646	0.537
Pb	0.798	0.492
Percentage of variance explained	46%	20%

Table 9. Varimax rotated principal components of heavy metals in sediments from the study area. *Extraction method:* Principal component analysis. *Rotation method:* Varimax with Kaiser normalization. Rotation converged in 3 iterations.

In PCA, variables are loaded with varimax rotation and analyzed using SPSS version 16.0 as given in Table 9. According to the PCA, two components were obtained for 19 elements. The first factor, with a value of 46%, has the highest explanatory power. The other four factors obtained explain 66% of the total variance. According to the rotated Component Matrix, the elements of Mg, Ti, Fe, V, Cr, Mn, Co, Ni, Zn, and Pb constituted component 1, representing a similar origin⁴⁰. Similarly, Si, As, and La constitute component 2, indicating that these metals are derived from different sources. These results are in good agreement with correlation analysis. Figure 8 shows the principal components of heavy metal of sediment.

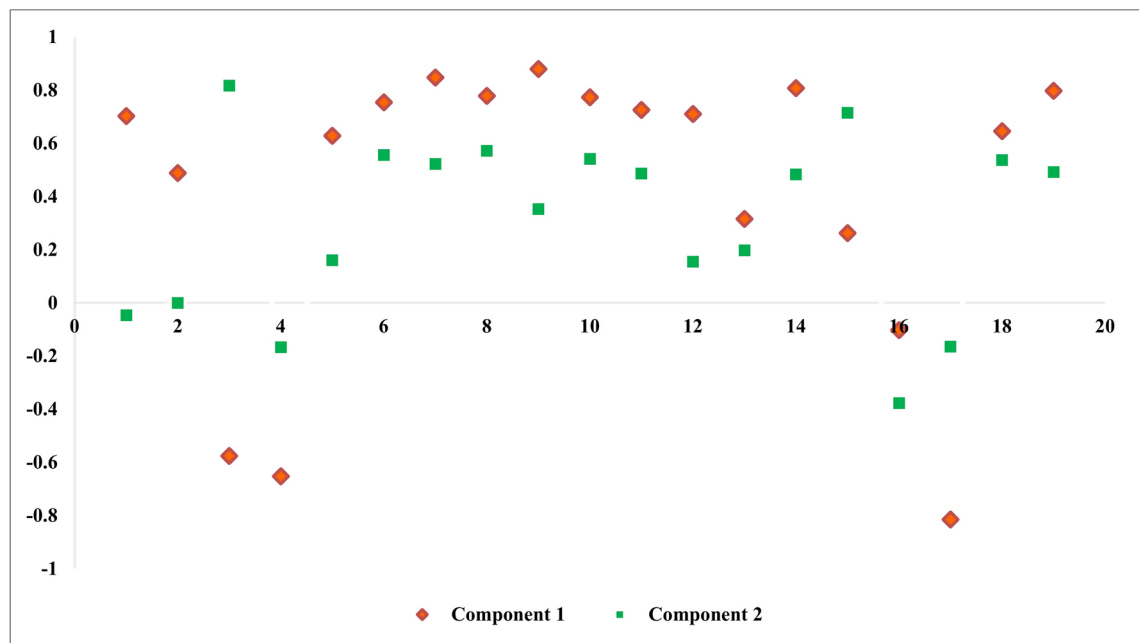


Fig. 8. Principal components of heavy metals of sediments.

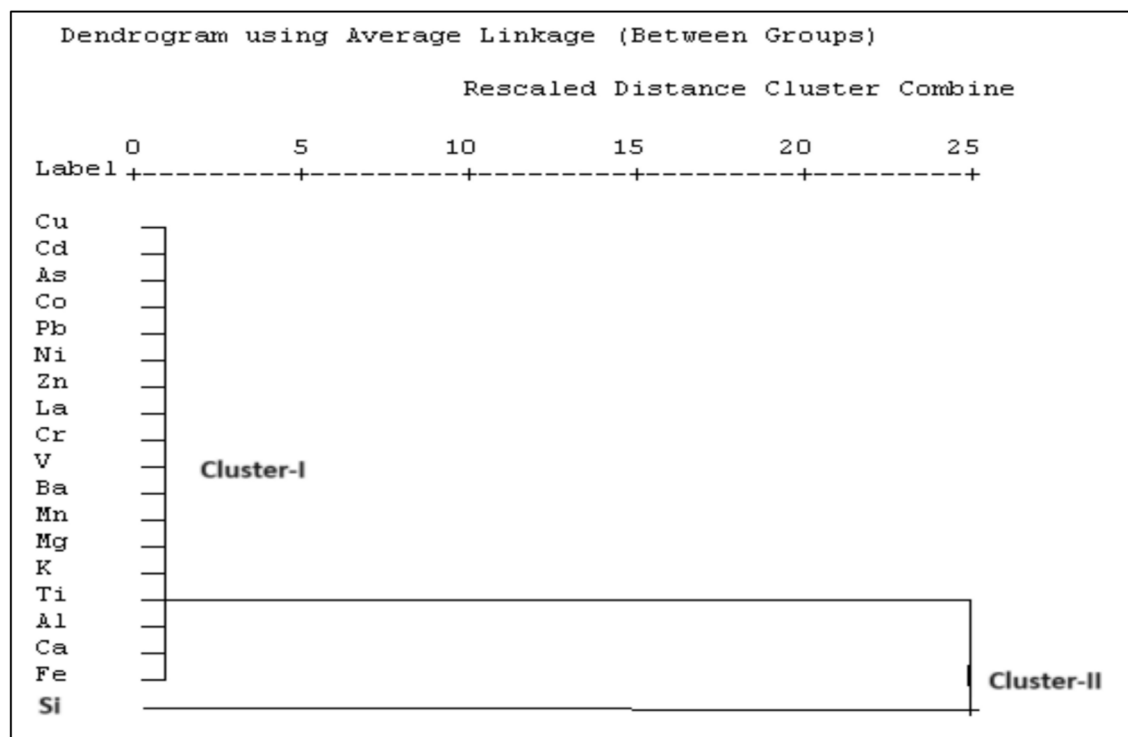


Fig. 9. Clustering of heavy metals of sediments.

Cluster analysis

Cluster analysis aims to identify a standard to classify variables based on inter-group differences and intra-group similarity. The data underwent normalization for cluster analysis. The present study employed the average linkage method and the Euclidean distance⁴¹. Figure 9 demonstrates the hierarchical dendrogram of the results. Figure 9 suggests two clusters: one containing Mg, As, Co, Ni, La, V, Ba, Mn, K, Ti, Al, Fe, Cu, Cd, Zn, and Pb, and the other consisting of Si; the former represents anthropogenic sources, while the latter stands for natural sources in the study area.

The statistical analyses conducted in this study included Pearson correlation, principal component analysis (PCA), and cluster analysis. For Pearson correlation, assumptions of linearity and homoscedasticity were considered, and the correlation coefficients were used to identify relationships between elements. PCA was applied to reduce dimensionality and identify significant components, with the assumptions of data normality and linear relationships between variables. For cluster analysis, data were normalized to ensure comparability. Validation included cross-checking results across methods, confirming consistency in grouping and component patterns.

Conclusion

The assessment likely involved collecting sediment samples from different places in the Ennore port area, analyzing the concentrations of heavy metals using atomic absorption spectroscopy (AAS), and comparing the results to established guidelines or background levels to evaluate the degree of pollution and potential risk associated with the heavy metal concentrations. The mean concentration of heavy metals was ranked in the following sequence of $\text{Si} > \text{Al} > \text{Fe} > \text{Ca} > \text{Ti} > \text{K} > \text{Mg} > \text{Mn} > \text{Ba} > \text{V} > \text{Cr} > \text{Zn} > \text{La} > \text{Ni} > \text{Pb} > \text{Co} > \text{As} > \text{Cd} > \text{Cu}$. The ranking indicates the relative abundance of these heavy metals in the sediments, with Si having the highest mean concentration and Cu the lowest among the metals analyzed. The concentration levels (mg kg^{-1}) of various elements exhibit the following ranges: 298–5987, 11,478–37,432, 115,987–224,978, 2985–9850, 3792–23,176, 540–49,434, 3597–56,502, 22.37–691, 11.5–198.29, 69.10–1227.61, 1.40–19.95, 11.48–38.63, BDL to 3.60, 11.04–87.99, 1.8–9.9, 1.1–11.2, 142.3–426.8, BDL to 214.7 and BDL to 30.7 for Mg, Al, Si, K, Ca, Ti, Fe, V, Cr, Mn, Co, Ni, Cu, Zn, As, Cd, Ba, La and Pb.

The enrichment factor analysis suggests a significant anthropogenic influence on the environment for Cr, Ca, Ti, V, and Cd, indicating that human activities have contributed to elevated levels of these metals beyond what would be expected from natural sources alone. Potential sources include industrial discharges, mining activities, use of chromium-containing products, and improper waste management practices. Values of the contamination factor (CF) indicate that the sediments were not contaminated with certain elements, suggesting that the concentrations of those elements are within acceptable or background levels and do not pose a risk to the environment or human health. The Igeo values for Co, Cr, Cu, Zn, Pb, and As fall within the range of 0–1, indicating that these metals are practically uncontaminated or only slightly contaminated in the sediments. Similar results were also obtained using the pollution load index (PLI).

The contamination was characterized using multivariate statistical analysis, including Pearson correlation analysis, principal component analysis, and cluster analysis. These analyses show that common sources and mutual dependence among certain metals (Al, Mg, Ca, Fe, Mn, Co, and Ni) suggest they may originate from similar pollution sources, undergo similar transport and transformation processes, or exhibit similar affinity for environmental matrices. Conversely, metals such as K (potassium), Cd (cadmium), and Ba (barium) were identified as coming from different sources and not exhibiting mutual dependence, indicating distinct contamination sources or behavior.

Heavy metal accumulation in beach sediments can have significant ecological consequences, including toxicity to aquatic organisms, bioaccumulation in food chains, and disruption of ecosystem functions. Elevated levels of metals such as Fe, Zn, and Ni can harm benthic organisms, reducing biodiversity and altering habitat structure. Moreover, bioaccumulation of toxic elements like Pb and As in higher trophic levels poses risks to both wildlife and human health. Future research should focus on long-term monitoring of heavy metal contamination, identifying potential sources, and assessing their bioavailability. Additionally, studies on the combined effects of multiple metals and the development of remediation strategies, such as phytoremediation or sediment washing, could provide practical solutions to mitigate environmental risks.

Data availability

Data is provided within the manuscript or supplementary information files.

Received: 5 November 2024; Accepted: 7 March 2025

Published online: 17 March 2025

References

- Li, Q. S. et al. Heavy metals in coastal wetland sediments of the Pearl River Estuary, China. *Environ. Pollut.* **149**, 158–164. <https://doi.org/10.1016/j.envpol.2007.01.006> (2007).
- Harikrishnan, N. et al. Assessment of heavy metal contamination in marine sediments of east coast of Tamil Nadu affected by different pollution sources. *Mar. Pollut. Bull.* **121**(1–2), 418–424. <https://doi.org/10.1016/j.marpolbul.2017.05.047> (2017).
- El-Sorogy, A. S. & Youssef, M. Assessment of heavy metal contamination in intertidal gastropod and bivalve shells from central Arabian Gulf coastline, Saudi Arabia. *J. Afr. Earth Sci.* **111**, 41–53. <https://doi.org/10.1016/j.jafrearsci.2015.07.012> (2015).
- El-Sorogy, A. S. & Attiah, A. Assessment of metal contamination in coastal sediments, seawaters and bivalves of the Mediterranean Sea coast, Egypt. *Mar. Pollut. Bull.* **101**, 867–871. <https://doi.org/10.1016/j.marpolbul.2015.11.017> (2015).
- Singovszka, E., Balintova, M., Demcak, S. & Pavlikova, P. Metal pollution indices of bottom sediment and surface water affected by acid mine drainage. *Metals* **7**, 284. <https://doi.org/10.3390/met7080284> (2017).
- Topaldemir, H., Taş, B., Yüksel, B. & Ustaoglu, F. Potentially hazardous elements in sediments and *Ceratophyllum demersum*: An ecotoxicological risk assessment in Miliç Wetland, Samsun, Türkiye. *Environ. Sci. Pollut. Res.* **30**, 26397–26416. <https://doi.org/10.1007/s11356-022-23937-2> (2022).
- Demircan, H., El-Sorogy, A. S., Al-Hashim, M. & Richiano, S. Taphonomic signatures on the pearl oyster *Pinctada* from Arabian Gulf, Saudi Arabia. *J. King Saud Univ. Sci.* **35**, 102870. <https://doi.org/10.1016/j.jksus.2023.102870> (2023).
- Alharbi, T. & El-Sorogy, A. S. Risk assessment of potentially toxic elements in agricultural soils of Al-Ahsa Oasis, Saudi Arabia. *Sustainability* **15**, 659. <https://doi.org/10.3390/su15010659> (2023).

9. Alharbi, T., Nour, H., Al-Kahtany, Kh., Giacobbe, S. & El-Sorogy, A. S. Sediment's quality and health risk assessment of heavy metals in the Al-Khafji area of the Arabian Gulf, Saudi Arabia. *Environ. Earth Sci.* **82**, 471. <https://doi.org/10.1007/s12665-023-11171-z> (2023).
10. Kahal, A. Y., El-Sorogy, A. S., Qaysi, S. I., Al-Hashim, M. H. & Al-Dossari, A. Environmental risk assessment and sources of potentially toxic elements in seawater of Jazan Coastal Area, Saudi Arabia. *Water* **15**, 3174. <https://doi.org/10.3390/w15183174> (2023).
11. Gao, X. L. & Li, P. M. Concentration and fractionation of trace metals in surface sediments of intertidal Bohai Bay, China. *Mar. Sci. Bull.* **64**, 1529–1536. <https://doi.org/10.1016/j.marpolbul.2012.04.026> (2012).
12. Islam, M. S. & Tanaka, M. Impacts of pollution on coastal and marine ecosystems including coastal and marine fisheries and approach for management: A review and synthesis. *Mar. Pollut. Bull.* **48**, 624–649. <https://doi.org/10.1016/j.marpolbul.2003.12.004> (2004).
13. Roussiez, V. et al. The fate of metals in coastal sediments of a Mediterranean flood dominated system: An approach based on total and labile fractions. *Estuar. Coast. Shelf Sci.* **92**, 486–495. <https://doi.org/10.1016/j.ecss.2011.02.009> (2011).
14. Rahman, M. A. & Ishiga, H. Trace metal concentrations in tidal flat coastal sediments, Yamaguchi Prefecture, southwest Japan. *Environ. Monit. Assess.* **184**, 5755–5771. <https://doi.org/10.1007/s10661-011-2379-x> (2012).
15. Nobis, E. P., Dilipan, E., Thangaradjou, T., Sivakumar, K. & Kannan, L. Geochemical and geo-statistical assessment of heavy metal concentration in the sediments of different coastal ecosystems of Andaman Islands, India. *Estuar. Coast. Shelf Sci.* **87**, 253–264. <https://doi.org/10.1016/j.ecss.2009.12.019> (2010).
16. Ustaoglu, F., Yüksel, B., Tepe, Y., Aydin, H. & Topaldemir, H. Metal pollution assessment in the surface sediments of a river system in Türkiye: Integrating toxicological risk assessment and source identification. *Mar. Pollut. Bull.* **203**, 116514. <https://doi.org/10.1016/j.marpolbul.2024.116514> (2024).
17. Pandian, P. K., Ramesh, S., Murthy, M. V., Ramachandran, S. & Thayumanavan, S. Shoreline changes and near shore processes along Ennore coast, east coast of South India. *J. Coast. Res.* **20**(3), 828–845. [https://doi.org/10.2112/1551-5036\(2004\)20\[828:SCA NSP\]2.0.CO;2](https://doi.org/10.2112/1551-5036(2004)20[828:SCA NSP]2.0.CO;2) (2004).
18. Karthikeyan, P., Marigoudar, S. R., Mohan, D., Naragjuna, A. & Sharma, K. V. Ecological risk from heavy metals in Ennore estuary, South East coast of India. *Environ. Chem. Ecotoxicol.* **2**, 182–193. <https://doi.org/10.1016/j.enceco.2020.09.004> (2020).
19. Yüksel, B. et al. Appraisal of metallic accumulation in the surface sediment of a fish breeding dam in Türkiye: A stochastic approach to ecotoxicological risk assessment. *Mar. Pollut. Bull.* **203**, 116488. <https://doi.org/10.1016/j.marpolbul.2024.116488> (2024).
20. Santhiya, G. et al. Metal enrichment in beach sediments from Chennai Metropolis, SE coast of India. *Mar. Pollut. Bull.* **62**, 2537–2542. <https://doi.org/10.1016/j.toxrep.2017.12.020> (2011).
21. Chandrasekaran, A. et al. Multivariate statistical analysis of heavy metal concentration in soils of Yelagiri Hills, Tamilnadu, India—Spectroscopic approach. *Spectrochim. Acta Part A* **137**, 589–600. <https://doi.org/10.1016/j.saa.2014.08.093> (2015).
22. Ravisankar, R. et al. Statistical assessment of heavy metal pollution in sediments of east coast of Tamilnadu using energy dispersive X-ray fluorescence spectroscopy (EDXRF). *Appl. Radiat. Isot.* **102**, 42–47. <https://doi.org/10.1016/j.apradiso.2015.03.018> (2015).
23. Harikrishnan, N., Chandrasekaran, A., Ravisankar, R. & Alagarsamy, R. Statistical assessment to magnetic susceptibility and heavy metal data for characterizing the coastal sediment of East coast of Tamilnadu, India. *Appl. Radiat. Isot.* **135**, 177–183. <https://doi.org/10.1016/j.apradiso.2018.01.030> (2018).
24. Sinex, S. A. & Helz, G. R. Regional geochemistry of trace elements in Chesapeake Bay sediments. *Environ. Geol.* **3**, 315–323. <https://doi.org/10.1007/BF02473521> (1981).
25. Selvaraj, K., Ram Mohan, V. & Szefer, P. Evaluation of metal contamination in coastal sediments of the Bay of Bengal, India: Geochemical and statistical approaches. *Mar. Pollut. Bull.* **49**, 174–185. <https://doi.org/10.1016/j.marpolbul.2004.02.006> (2004).
26. Turekian, K. K. & Wedepohl, K. H. Distribution of the elements in some major units of the Earth's crust. *Geol. Soc. Am. Bull.* **72**, 175–192. [https://doi.org/10.1130/0016-7606\(1961\)72\[175:DOTEIS\]2.0.CO;2](https://doi.org/10.1130/0016-7606(1961)72[175:DOTEIS]2.0.CO;2) (1961).
27. Zhang, J. & Liu, C. L. Riverine composition and estuarine geochemistry of particulate metals in China—weathering features, anthropogenic impact and chemical fluxes. *Estuar. Coast. Shelf Sci.* **54**, 1051–1070. <https://doi.org/10.1006/ecss.2001.0879> (2002).
28. Feng, H., Han, X., Zhang, W. & Yu, L. A preliminary study of heavy metal contamination in Yangtze River inter tidal zone due to urbanization. *Mar. Pollut. Bull.* **49**, 910–915. <https://doi.org/10.1016/j.marpolbul.2004.06.014> (2004).
29. Aggarwal, M., Anbukumar, S. & Vijaya Kumar, T. Measurement of heavy metals content in suspended sediment of Ganges river using atomic absorption spectrometry. *MAPAN* **39**, 913–930. <https://doi.org/10.1007/s12647-024-00771-0> (2024).
30. Cheng, H. & Hu, Y. Lead (Pb) isotopic fingerprinting and its applications in lead pollution studies in China: A review. *Environ. Pollut.* **158**, 1134–1146. <https://doi.org/10.1016/j.envpol.2009.12.028> (2010).
31. Muller, G. Schwermetalle in den sedimenten des Rheins—VeränderungenSeit. *Umschau* **24**, 778–783 (1979).
32. Yüksel, B., Ustaoglu, F., Tokarli, C. & Islam, M. S. Ecotoxicological risk assessment for sediments of Çavuşlu stream in Giresun, Turkey: Association between garbage disposal facility and metallic accumulation. *Environ. Sci. Pollut. Res.* **29**, 17223–17240. <https://doi.org/10.1007/s11356-021-17023-2> (2022).
33. Aggarwal, M., Anbukumar, S. & Vijaya Kumar, T. Analysis and pollution assessment of heavy metals in suspended solids of the middle stretch of river Ganga between Kanpur to Prayagraj, U.P., India. *Sādhanā* **48**(257), 01–13. <https://doi.org/10.1007/s12046-023-02325-7> (2023).
34. Hakanson, L. An ecological risk index for aquatic pollution control. A sedimentological approach. *Water Res.* **14**, 975–1001. [https://doi.org/10.1016/0043-1354\(80\)90143-8](https://doi.org/10.1016/0043-1354(80)90143-8) (1980).
35. Aggarwal, M., Anbukumar, S. & Vijaya Kumar, T. Heavy metals concentrations and risk assessment in the sediment of Ganga River between Kanpur and Prayagraj U.P., India. *Sādhanā* **47**(195), 01–11. <https://doi.org/10.1007/s12046-022-01972-6> (2022).
36. Hosono, T. et al. Decline in heavy metal contamination in marine sediments in Jakarta Bay, Indonesia due to increasing environmental regulations. *Estuar. Coast. Shelf Sci.* **92**, 297–306. <https://doi.org/10.1016/j.ecss.2011.01.010> (2011).
37. Tomlinson, D. C., Wilson, J. G., Harris, C. R. & Jeffrey, D. W. Problems in the assessment of heavy metals in estuaries and the formation pollution index. *Helgol. Mar. Res.* **33**, 566–575. <https://doi.org/10.1007/BF02414780> (1980).
38. Yalcin, F. Data analysis of beach sands' chemical analysis using multivariate statistical methods and heavy metal distribution maps: The case of moonlight beach sands, Kemer, Antalya, Turkey. *Symmetry* **12**(9), 1538. <https://doi.org/10.3390/sym12091538> (2020).
39. Zhang, Y., Hu, X. & Yu, T. Distribution and risk assessment of metals in sediments from Taihu Lake, China using multivariate statistics and multiple tools. *Bull. Environ. Contam. Toxicol.* **89**, 1009–1015. <https://doi.org/10.1007/s00128-012-0784-7> (2012).
40. Khan, R. et al. Spatial and multi-layered assessment of heavy metals in the sand of Cox's-Bazar beach of Bangladesh. *Reg. Stud. Mar. Sci.* **16**, 171–180. <https://doi.org/10.1016/j.rsma.2017.09.003> (2017).
41. Sohrabizadeh, Z., Sodaeizadeh, H., Hakimzadeh, M. A., Taghizadeh-Mehrjardi, R. & Ghanei Bafghi, M. J. A statistical approach to study the spatial heavy metal distribution in soils in the Kushk Mine, Iran. *Geosci. Data J.* **10**(3), 315–327. <https://doi.org/10.1002/gdj3.175> (2023).
42. Abbasi, K. & Mirekhtiary, F. Heavy metals and natural radioactivity concentration in sediments of the Mediterranean Sea coast. *Mar. Pollut. Bull.* **154**, 111041. <https://doi.org/10.1016/j.marpolbul.2020.111041> (2020).
43. Duman, M., Kucuksezgin, F., Atalar, M. & Akcali, B. Geochemistry of the northern Cyprus (NE Mediterranean) shelf sediments: Implications for anthropogenic and lithogenic impact. *Mar. Pollut. Bull.* **64**, 2245–2250. <https://doi.org/10.1016/j.marpolbul.2012.06.025> (2012).

44. Pappa, F. K. et al. Radioactivity and metal concentrations in marine sediments associated with mining activities in Ierissos Gulf, North Aegean Sea, Greece. *Appl. Radiat. Isot.* **116**, 22–33. <https://doi.org/10.1016/j.apradiso.2016.07.006> (2016).
45. Akozcan, S. & Gorgun, A. U. Trace metal and radionuclide pollution in marine sediments of the Aegean Sea (Izmir Bay and Didim). *Environ. Earth Sci.* **69**(7), 2351–2355. <https://doi.org/10.1007/s12665-012-2064-6> (2013).
46. Maanan, M. et al. Environmental and ecological risk assessment of heavy metals in sediments of Nador lagoon, Morocco. *Ecol. Indic.* **48**, 616–626. <https://doi.org/10.1016/j.ecolind.2014.09.034> (2015).
47. Tornero, V., Arias, A. M. & Blasco, J. Trace element contamination in the Guadalquivir River Estuary ten years after the Aznalcollar mine spill. *Mar. Pollut. Bull.* **86**(1–2), 349–360. <https://doi.org/10.1016/j.marpolbul.2014.06.044> (2014).
48. Resongles, E. et al. Persisting impact of historical mining activity to metal (Pb, Zn, Cd, Tl, Hg) and metalloid (As, Sb) enrichment in sediments of the Gardon River, Southern France. *Sci. Total Environ.* **481**, 509–521. <https://doi.org/10.1016/j.scitotenv.2014.02.078> (2014).
49. Ben Amor, R., Yahyaoui, A., Abidi, M., Chouba, L. & Gueddari, M. Bioavailability and assessment of metal contamination in surface sediments of rades-hamam lif coast, around meliane river (Gulf of Tunis, Tunisia, Mediterranean Sea). *J. Chem.* **2019**, 01–11. <https://doi.org/10.1155/2019/4284987> (2019).
50. Kontaş, A., Uluturhan, E., Akcalı, İ., Darılmaz, E. & Altay, O. Spatial distribution patterns, sources of heavy metals, and relation to ecological risk of surface sediments of the Cyprus northern shelf (Eastern Mediterranean). *Environ. Forensic* **16**, 264–274. <https://doi.org/10.1080/15275922.2015.1059386> (2015).
51. Jayaprakash, M. et al. Bioaccumulation of metals in fish species from water and sediments in macrotidal Ennore creek, Chennai, SE coast of India: A metropolitan city effect. *Ecotoxicol. Environ. Saf.* **120**, 243–255. <https://doi.org/10.1016/j.ecoenv.2015.05.042> (2015).
52. Dhanakumar, S., Solaraj, G. & Mohanraj, R. Heavy metal partitioning in sediments and bioaccumulation in commercial fish species of three major reservoirs of river Cauvery delta region, India. *Ecotoxicol. Environ. Saf.* **113**, 145–151. <https://doi.org/10.1016/j.ecoenv.2014.11.032> (2015).
53. Lakshmanasenthil, S. et al. Harmful metals concentration in sediments and fishes of biologically important estuary, Bay of Bengal. *J. Environ. Health Sci. Eng.* **11**(1), 33. <https://doi.org/10.1186/2052-336X-11-33> (2013).
54. Raj, S., Jee, P. K. & Panda, C. R. Textural and heavy metal distribution in sediments of Mahanadi estuary, East coast of India. *Indian J. Mar. Sci.* **42**(3), 370–374 (2013).
55. Kumar, S. P. & Patterson Edward, J. K. Assessment of metal concentration in the sediment cores of Manakudy estuary, southwest coast of India. *Indian J. Mar. Sci.* **38**(2), 235–248 (2009).
56. Jitar, O., Oros, A., Teodosiu, C., Plavan, G. & Nicoara, M. Bioaccumulation of heavy metals in marine organisms from the Romanian sector of the Black Sea. *New Biotechnol.* **32**(3), 369–378. <https://doi.org/10.1016/j.nbt.2014.11.004> (2015).
57. Qiu, Y. W. Bioaccumulation of heavy metals both in wild and mariculture food chains in Daya Bay, South China. *Estuar. Coast. Shelf Sci.* **163**, 07–14. <https://doi.org/10.1016/j.ecss.2015.05.036> (2015).
58. Cevik, U. et al. Assessment of metal element concentration in mussel (*M. galloprovincialis*) in Eastern Black Sea, Turkey. *J Hazard Mater.* **160**, 396–401. <https://doi.org/10.1016/j.jhazmat.2008.03.010> (2008).
59. Yan, Y. et al. Background determination, pollution assessment and source analysis of heavy metals in estuarine sediments from Quanzhou Bay, Southeast China. *CATENA* **187**, 104322. <https://doi.org/10.1016/j.catena.2019.104322> (2020).
60. Yang, H. J. et al. Organic matter and heavy metal in river sediments of southwestern coastal Korea: Spatial distributions, pollution, and ecological risk assessment. *Mar. Pollut. Bull.* **159**, 111466. <https://doi.org/10.1016/j.marpolbul.2020.111466> (2020).
61. Hwang, D. W. et al. Spatial distribution and pollution assessment of metals in intertidal sediments, Korea. *Environ. Sci. Pollut. Res.* **26**(19), 19379–19388. <https://doi.org/10.1007/s11356-019-05177-z> (2019).
62. Du Laing, G. et al. Heavy metal mobility in intertidal sediments of the Scheldt estuary: Field monitoring. *Sci. Tot. Environ.* **407**(8), 2919–2930. <https://doi.org/10.1016/j.scitotenv.2008.12.024> (2009).
63. Manju, M. N. et al. Trace metal distribution in the sediment cores of mangrove ecosystems along northern Kerala coast, south-west coast of India. *Mar. Pollut. Bull.* **153**, 110946. <https://doi.org/10.1016/j.marpolbul.2020.110946> (2020).
64. Fan, H. et al. Assessment of heavy metals in water, sediment and shellfish organisms in typical areas of the Yangtze River Estuary, China. *Mar. Pollut. Bull.* **151**, 110864. <https://doi.org/10.1016/j.marpolbul.2019.110864> (2020).
65. Wang, X., Liu, B. & Zhang, W. Distribution and risk analysis of heavy metals in sediments from the Yangtze River Estuary, China. *Environ. Sci. Pollut. Res.* **27**, 10802–10810. <https://doi.org/10.1007/s11356-019-07581-x> (2020).
66. Díaz-de Alba, M., Galindo-Riano, M. D., Casanueva-Marceno, M. J., García-Vargas, M. & Kosore, C. M. Assessment of the metal pollution, potential toxicity and speciation of sediment from Algeciras Bay (South of Spain) using chemometric tools. *J. Hazard. Mater.* **190**, 177–187. <https://doi.org/10.1016/j.jhazmat.2011.03.020> (2011).

Acknowledgements

The authors express their gratitude to the Coastal Environmental Engineering Division (CEE) of the National Institute of Ocean Technology (NIOT), NIOT Campus, Pallikaranai, Chennai – 600100, Tamil Nadu, India, for their valuable collaboration, insights, and contributions.

Author contributions

D. Rajendiran: Writing—original draft, visualization, validation, methodology, investigation, formal analysis, conceptualization. N. Harikrishnan: Writing—review and editing, resources, methodology, conceptualization. K. Veeramuthu: Writing—review and editing, validation, supervision, resources, methodology, conceptualization, project administration.

Declarations

Competing interests

The authors declare no competing interests.

Additional information

Correspondence and requests for materials should be addressed to K.V.

Reprints and permissions information is available at www.nature.com/reprints.

Publisher's note Springer Nature remains neutral with regard to jurisdictional claims in published maps and institutional affiliations.

Open Access This article is licensed under a Creative Commons Attribution-NonCommercial-NoDerivatives 4.0 International License, which permits any non-commercial use, sharing, distribution and reproduction in any medium or format, as long as you give appropriate credit to the original author(s) and the source, provide a link to the Creative Commons licence, and indicate if you modified the licensed material. You do not have permission under this licence to share adapted material derived from this article or parts of it. The images or other third party material in this article are included in the article's Creative Commons licence, unless indicated otherwise in a credit line to the material. If material is not included in the article's Creative Commons licence and your intended use is not permitted by statutory regulation or exceeds the permitted use, you will need to obtain permission directly from the copyright holder. To view a copy of this licence, visit <http://creativecommons.org/licenses/by-nc-nd/4.0/>.

© The Author(s) 2025